

Peatland development reconstruction and complex biological responses to permafrost thawing in Western Siberia

Agnieszka Halaś¹, Mariusz Lamentowicz², Milena Obremska³, Dominika Łuców¹, Michał Słowiński¹

¹ Department of Past Landscape Dynamics, Institute of Geography and Spatial Organization Polish Academy of Sciences, Warsaw, 00-818, Poland

² Climate Change Ecology Research Unit, Faculty of Geographical and Geological Sciences, Adam Mickiewicz University, Poznań, 61-680, Poland

³ Institute of Geological Sciences, Polish Academy of Sciences, Research Centre in Warsaw, Warszawa, 00-818, Poland

Correspondence to: Agnieszka Halaś (aj.halas@twarda.pan.pl)

Abstract. Western Siberian peatlands are among the largest peatland complexes in the world and play a crucial role in regulating the global climate. However, a lack of long-term, multi-proxy studies comprehensively examining the interactions between permafrost thaw and peatland ecosystems in Western Siberia hinders the ability to predict their response to future climate change. This research covers two centuries of the Khanymei peatlands history, situated within the discontinuous permafrost zone. In this study, a multi-proxy analysis (testate amoebae, plant macrofossil, pollen, micro- and macrocharcoal, loss on ignition) was conducted on two peat cores – one from a peat plateau and another from the edge of a thermokarst lake. We inferred peatland drying from the end of the Little Ice Age. The elevated peat plateau facilitated the aggradation of permafrost, which began to thaw in recent decades due to rising air temperatures, increasing peat moisture. The lake edge was the most dynamic part of the peatland, where more notable changes in hydrology, vegetation, and microbial composition occurred. Thawing led to significant *Sphagnum* growth and a shift in the testate amoebae community structure. We reconstructed the effects of permafrost thawing that resulted in a substantial but short-term and local increase in peat and carbon accumulation and an increased abundance of fungal communities. Our study reveals that thaw-induced terrain subsidence was subtle and spatially variable, yet these localized surface changes triggered complex hydrological, vegetational, and microbial responses, highlighting the nonlinear and multifaceted nature of permafrost degradation. The advantage of our research lies in the utilization of multi-proxy high-resolution palaeoecological techniques, enabling us to monitor even relatively minor permafrost transformations and identify early warning signals of climate-induced impacts on this invaluable ecosystem. We anticipate that further warming will contribute to the occurrence of these processes on a larger scale in Western Siberian peatlands, potentially significantly impacting ecosystem conditions and the global climate.

1. Introduction

Peatlands of Western Siberian Lowlands cover 592 440 km², with many underlain by permafrost (Sheng et al., 2004). Since the early Holocene, this region has been a carbon dioxide sink and during the last 11 ka has accumulated 70.2 Pg C, ~26% of all terrestrial carbon stored (Smith et al., 2004). Around half of this soil organic carbon is accumulated in permafrost-affected peat, making it vulnerable to climate change (Hugelius et al., 2020). Recent studies suggest that since 1979 CE, the Arctic has experienced warming almost four times as fast as lower latitudes due to a phenomenon known as Arctic amplification (Hantemirov et al., 2022; Rantanen et al., 2022; IPCC, 2023). Arctic warming accelerates permafrost thawing and significantly impacts Western Siberia, particularly peatland ecosystems (Hantemirov et al., 2022).

Permafrost peatlands are a unique environment with complex relationships between hydrological conditions, vegetation structures, peat accumulation and related carbon balance. The complexity of these interactions intensifies with permafrost thawing; however, many aspects remain unclear. During phases of stable permafrost, cold conditions make organic carbon

relatively inactive (Swindles et al., 2015). Increased temperatures impact permafrost peatlands by inducing permafrost thaw, which leads to the release of little decomposed organic matter, and by triggering the activation of anaerobic decay processes (Jeong et al., 2018; Karlsson et al., 2021). The microbial decomposition of accumulated peat contributes to an increase in carbon dioxide (CO₂) and methane (CH₄) emissions from peatlands, which have positive feedback on climate (Jeong et al., 2018).

Thawing permafrost leads to an increase in the moisture content of the overlying peat layer. The increased water volume in circulation contributes to hydrologic modifications, especially in surface and subsurface hydrology of permafrost areas (Walvoord and Kurylyk, 2016). The enhanced wetness alters the thermal conductivity of peat (Kujala et al., 2008), diminishing peat insulation properties and facilitating easier and deeper heat penetration of underlying permafrost. This process creates a positive feedback loop, leading to further permafrost thawing and the amplification of climate warming (Schuur et al., 2015). A clear indication of thawing is an increase in active layer thickness (ALT), which has changed by 0.4 m in the Russian Arctic since 1990 CE (Smith et al., 2022). The changes in ALT lead to terrain subsidence (Ekici et al., 2019; O'Neill et al., 2023) and affect thermokarst lakes, a prominent feature of the Western Siberia landscape (Kremenetski et al., 2003). Initially, increased water supply leads to lake formation and expansion (Fewster et al., 2022; Luoto and Seppälä, 2003). However, new outflow channels created by continued permafrost degradation and increased evapotranspiration contribute to rapid lake drainage and disappearance (Webb and Liljedahl, 2023). This trend is visible especially in discontinuous and sporadic permafrost zones (Smith et al., 2005), where further thawing may shift these regions from surface water-dominated to groundwater-dominated systems (Frey et al., 2007).

The processes that are now observed in the Arctic-Boreal ecosystems are complex, scale-dependent, and determined by local conditions. The surface of permafrost peatlands often consists of microhabitats (palsa/peat plateau - depression), which are a result of complex interactions between vegetation growth, moisture, decomposition, peat accumulation, and permafrost (Nungesser, 2003; Rydin and Jeglum, 2013). The heterogeneous nature of permafrost peatlands facilitates the occurrence of various processes within short distances, which makes it difficult to predict how these peatlands will react to current warming (Sim et al., 2021). Numerous studies have emphasized their crucial role in global climate dynamics; however, these ecosystems remain unrepresented in climate models (Fewster et al., 2022; Sim et al., 2021; Swindles et al., 2015; Zhang et al., 2022).

The hydrological conditions of permafrost-affected peatlands following thaw will vary widely, and the trajectory of these changes is uncertain (Sim et al., 2021). As permafrost thaws, the destabilization of characteristic landscape features will lead to the formation of water-saturated areas with melting ice and elevated seasonal water tables (Sannel and Kuhry, 2011; Swindles et al., 2015). However, increased temperatures will also drive higher evapotranspiration rates, potentially causing drier conditions in certain areas depending on the microhabitat type and the season (Lawrence et al., 2015; Spiller et al., 2024). Bogs and fens may experience drier surface layers, particularly in summer, while faster drainage could occur following the thaw of ground ice (Sannel and Kuhry, 2011; Spiller et al., 2024). Observations already show that northern peatlands respond in diverse ways to warming, with no single, uniform trend of either wetting or drying (Sim et al., 2021; Zhang et al., 2022).

Many studies have indicated that permafrost thaw will have a beneficial effect on vegetation productivity in Arctic-Boreal ecosystems, causing so-called *greening* (Myers-Smith et al., 2020) and increased carbon accumulation (Heffernan et al., 2020). Greening dominates in northern regions, in Western Siberia above 64°N (Miles and Esau, 2016). Regions further south experience *browning*, characterized by decreased productivity (Miles and Esau, 2016; Phoenix and Bjerke, 2016), associated with disturbances such as drought (Magnússon et al., 2023), water stress (Li et al., 2021), insect outbreaks (Kurz et al., 2008) or wildfires (Zoltai et al., 1998). The transitional zone between these *greening*-dominated and *browning*-dominated regions is of particular interest, as it may reflect early signals of ecosystem change. Our study focuses on the permafrost peatlands, located within this transitional zone, which may indicate that some parts of these peatlands have already surpassed the period of post-thaw beneficial enhanced plant productivity (Ogden et al., 2023; Phoenix and Bjerke, 2016).

Palaeoecological reconstructions provide invaluable information about past environmental conditions and ecosystem responses to past climate changes (Bottjer, 2016). This is particularly important because palaeoecological records cover a much longer timeframe than observational data and, when using a multi-proxy approach, can offer a more comprehensive understanding of past ecosystem dynamics (Chambers and Charman, 2004). Different palaeoecological proxies can provide insights into peatland moisture conditions (Halaš et al., 2023; Lamentowicz et al., 2015), local (Feurdean et al., 2019; Volkova et al., 2019), and regional vegetation composition (De Klerk et al., 2009; Novenko et al., 2023) and fire activity (Conedera et al., 2009; Feurdean et al., 2019).

Western Siberian peatlands have been the subject of a spare number of studies comprehensively reconstructing their history (Beilman et al., 2009; Feurdean et al., 2019, 2020, 2022; Kurina et al., 2023; Lamentowicz et al., 2015; Peteet et al., 1998; Philben et al., 2014; Tikhonravova et al., 2023; Willis et al., 2015). Due to the vast area and challenging accessibility of Western Siberian peatlands, Russian paleoecologists began studying them in the early 20th century (Kremenetski et al., 2003). Most early research focused on peatland distribution, peat thickness, basal age, and fossil pollen and plant records (Kremenetski et al., 2003; Neustadt, 1967). More recent studies have focused on multi-proxy analyses (e.g., Feurdean et al., 2019; Kurina et al., 2023; Lamentowicz et al., 2015), vegetation reconstructions (Peteet et al., 1998; Philben et al., 2014; Tikhonravova et al., 2023), and carbon accumulation (Beilman et al., 2009). Fire history has also been investigated (Feurdean et al., 2020, 2022), while testate amoebae have been used to reconstruct peatland hydrology in only a few studies (Feurdean et al., 2020; Kurina et al., 2023; Lamentowicz et al., 2015; Willis et al., 2015). Due to the large area of the region, in situ data are primarily available from more accessible areas, emphasizing the need for further investigation. Despite an increase in publications on Western Siberian peatlands in recent decades, research in this region is expected to decline in the near future due to ongoing accessibility challenges (Schoor et al., 2024). Our research presents new insight into the history of peatlands in a poorly explored region of Western Siberia. The presented data covers an important period from the end of the Little Ice Age to modern times, providing information on how Khanymei peatland ecosystems and peatland's microhabitats have responded to recent warming.

Our study aimed to reconstruct past environmental changes on peatlands from the discontinuous permafrost zone based on two cores. The main objectives were to (1) reconstruct the 200-year history of Khanymei peatlands using a multi-proxy approach; (2) analyse differences in biological responses of peatland microhabitats to permafrost thaw; and (3) identify patterns of the progressive permafrost degradation in discontinuous permafrost zone.

2. Study area

The study area is located near Khanymei (Yamal-Nenets Autonomous District) (Fig. 1). The studied peatlands are situated at the northern border of the boreal forest taiga zone, which includes woodlands and open stands (Fig. 1B). Due to the presence of discontinuous permafrost, palsa and peat plateaus (with a frozen core) surrounded by thermokarst lakes are a characteristic feature of the study area.

The studied region has a boreal climate with short, cool summers and long, cold, snowy winters (Peel et al., 2007). The mean annual air temperature is between -3.5 and -6°C, January air temperature ranges from -22 to -24°C, and July from 15.5 to 17°C (Trofimova and Balybina, 2014). The average annual precipitation in the Khanymei area is 436 mm (Kluge et al., 2021). Siberia stands out as one of the regions experiencing the most pronounced warming worldwide in recent years, and modern climate models project that this trend will continue (Groisman et al., 2013; Hantemirov et al., 2022). There has been a notable rise in hot extremes and a decline in cold extremes over recent decades (Seneviratne et al., 2021). Additionally, precipitation patterns have been altered significantly, with intensified heavy rainfall during the warm season (Seneviratne et al., 2021) and increased precipitation and snow water equivalent during the cold season (Bulygina et al., 2011; Groisman et al., 2013).

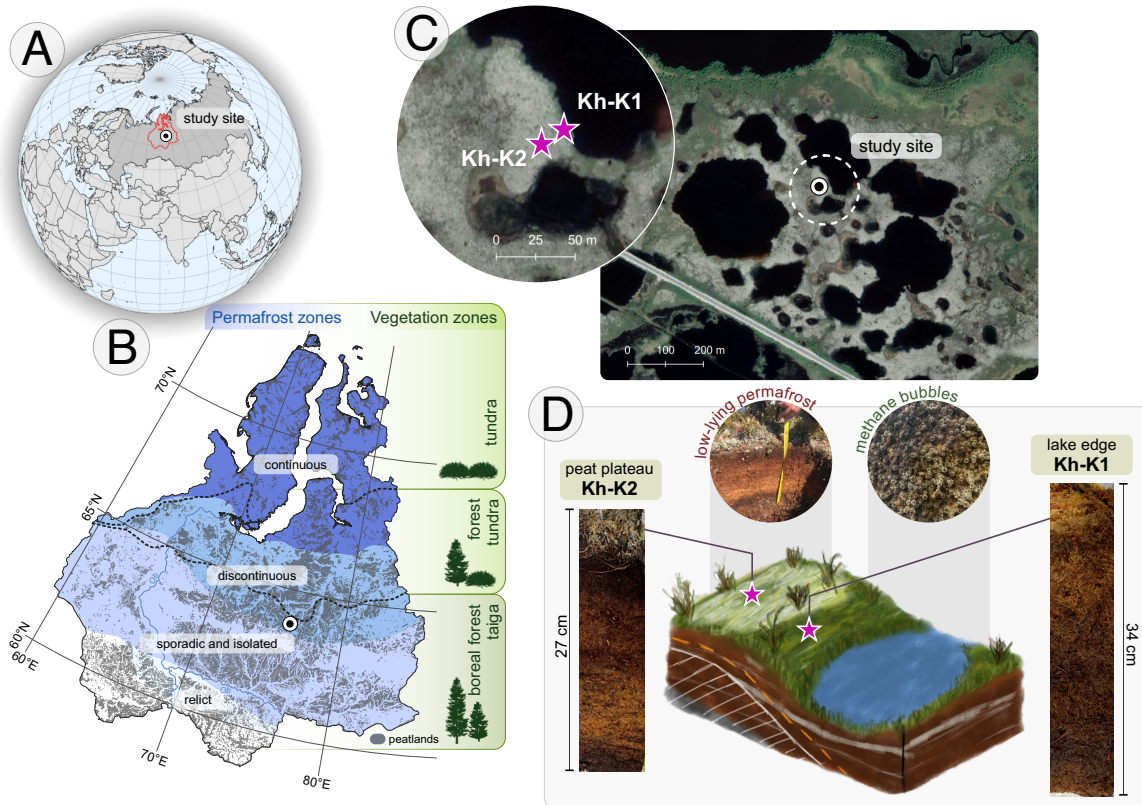


Figure 1 Study area: A) location of West Siberian Lowland (WLS); B) WLS – permafrost extent based on Brown et al. (1997), peatland extend based on Sheng et al. (2004) and vegetation zones based on Davydova and Rakovskaya (1990); C) location of coring sites (background map source: © Google Earth 2015); D) illustration of the peat plateau-lake edge microhabitat on study site with photos of peat cores.

The northern border of the boreal forest taiga zone is characterized by coniferous pine (*Pinus sylvestris* and *Pinus sibirica*) and larch (*Larix sibirica*) open forests (Safronova and Yurkovskaya, 2019). The palsas and peat plateaus are covered by moss-lichen mosaics with a presence of dwarf shrubs (e.g. *Rhododendron tomentosum*) and dwarf birch (*Betula nana*) (Safronova and Yurkovskaya, 2019; Volkova et al., 2019). Additionally, in permafrost peatland ecosystems in the Khanymei region, lichens (genera *Cladonia*) occupy 70-80% of peatland surface and form a unique type of lichen peat (Volkova et al., 2019).

Peatlands started to form in Western Siberia in the early Holocene, between 11,000 and 10,000 cal BP (Kremenetski et al., 2003). Even though Western Siberia lacked ice sheet cover during the last glacial period, the initiation of peatlands formation did not occur until the post-glacial warming of this region (Abe-Ouchi et al., 2015). Unfavourable conditions for peat accumulation during the glacial period were caused by a limited moisture influx from the North Atlantic due to the spread of the ice cover in the Arctic Ocean and the Siberian High (Velichko et al., 2011). According to Alexandrov et al. (2016), summer dryness-induced moisture imbalance was an essential factor preventing the formation of *Sphagnum*-dominated peatlands during the glacial period in this part of Siberia. Peatlands in the Khanymei region were mostly formed on sandy and silty sediments, and peat deposits are usually 0.1-1.4 m deep (Raudina et al., 2017; Velichko et al., 2011).

2.1. Permafrost development in Western Siberia

The permafrost in Western Siberia was mainly developed in Late Pleistocene (18-27 ka BP), and during the most favourable conditions, the southern limit reached 48-49°N (Duchkov, 2006). The early Holocene warming led to a northward shift of the border up to 60°N. During the Subatlantic cooling (2-1.3 ka BP), an epigenetic permafrost aggradation started, and peat deposits accumulated after deglaciation were first to freeze (Kondratjeva et al., 1993). The good insulating properties of *Sphagnum* mosses allowed frost to persist during warmer seasons and extend into the deeper mineral layers. This process led

to the development of permanently frozen peatlands and the formation of palsas due to the cryogenic lifting of the peatland's surface (Martini et al., 2007). The characteristic feature of discontinuous permafrost is thermokarst lakes, which developed in the Khanymei area around 2.5 ka BP under stable permafrost conditions (Martini et al., 2007; Raudina et al., 2017).

150 **3. Methods and materials**

155 **3.1. Coring and sediment sub-sampling**

Two peat cores with a diameter of 10 × 10 cm were collected from Khanymei permafrost peatlands at the turn of June and July 2019. Cores were extracted from the peat plateau-lake edge complex 5 m apart from each other (Fig. 1C). The core Kh-K1 (34 cm, 63.7856° N, 75.6438° E) was taken from the lake edge and Kh-K2 (27 cm, 63.7855° N, 75.6434° E) from a peat plateau. The peat monoliths were extracted using a knife. The Kh-K2 core was sampled until the frozen peat was reached. Each peat core was then sub-sampled in 1-cm resolution (except for 0–2 cm in Kh-K2) for testate amoebae (sample volume: 3 cm³), pollen and microcharcoal (1 cm²), macrocharcoal (2 cm²), plant macrofossils (4 cm³), and loss on ignition (1 cm³) analyses.

160 **3.2. Chronology and peat accumulation rate**

Eight samples from Kh-K1 and five from Kh-K2 of terrestrial plant macrofossils were selected for dating (Table 1). Cores chronology was based on ¹⁴C dating using an Accelerator Mass Spectrometer (AMS) in the Poznań Radiocarbon Laboratory. The radiocarbon dates were calibrated with IntCal20 (Reimer et al., 2020) and NH1 post-bomb (Hua et al., 2013) atmospheric curves (Fig. 2). For models calculation with 1-cm resolution, the *P_Sequence* function with parameters k0 = 10 and log10(k/k0) = 1 was applied. One calendar year representing the date of coring 2019.6 at a depth of 0 cm, was introduced to the model. The age-depth models were calculated using the OxCal v4.4.4 software (Ramsey, 2001). The peat accumulation rate (PAR, mm·yr⁻¹) was calculated by dividing the sample thickness (mm) by the age difference between the top and bottom limits of the sample (CE years).

Table 1 Radiocarbon (¹⁴C) dates from peat cores Kh-K1 and Kh-K2

Core	Depth (cm)	Lab Number	¹⁴ C age or F ¹⁴ C*	Material dated	Calibrated age (CE)	2σ range modelled age range (CE)
Kh-K1	2-3	Poz-150655	<i>101.58 ± 0.34</i>	<i>Sphagnum steams</i>	2009	2009-2009
	5-6	Poz-150725	<i>103.83 ± 0.32</i>	<i>Sphagnum steams</i>	2008	2007-2008
	9-10	Poz-150726	<i>106 ± 0.33</i>	<i>Sphagnum steams</i>	2006	2005-2007
	14-15	Poz-150728	<i>108.5 ± 0.39</i>	<i>Sphagnum steams</i>	2002	2000-2003
	19-20	Poz-150663	<i>111.55 ± 0.36</i>	<i>Sphagnum steams</i>	1996	1994-1997
	24-25	Poz-150664	<i>119.86 ± 0.37</i>	<i>Sphagnum steams</i>	1986	1984-1987
	30-31	Poz-157591	<i>102.87 ± 0.28</i>	<i>Sphagnum steams</i>	1957	1956-1957
	33-34	Poz-157563	<i>104.75 ± 0.31</i>	<i>Sphagnum steams</i>	1956	1955-1956
Kh-K2	6-7	Poz-150837	<i>125.66 ± 0.45</i>	<i>Sphagnum steams</i>	1975	1959-1982
	10-11	Poz-150665	105 ± 30	<i>Sphagnum steams</i>	1930	1902-1954
	15-16	Poz-150838	25 ± 30	<i>Sphagnum steams</i>	1894	1822-1920
	20-21	Poz-150666	105 ± 30	<i>Sphagnum steams</i>	1860	1756-1901
	26-27	Poz-150839	90 ± 30	<i>Sphagnum steams</i>	1814	1692-1875

* postbomb F¹⁴C values are shown in *italics*

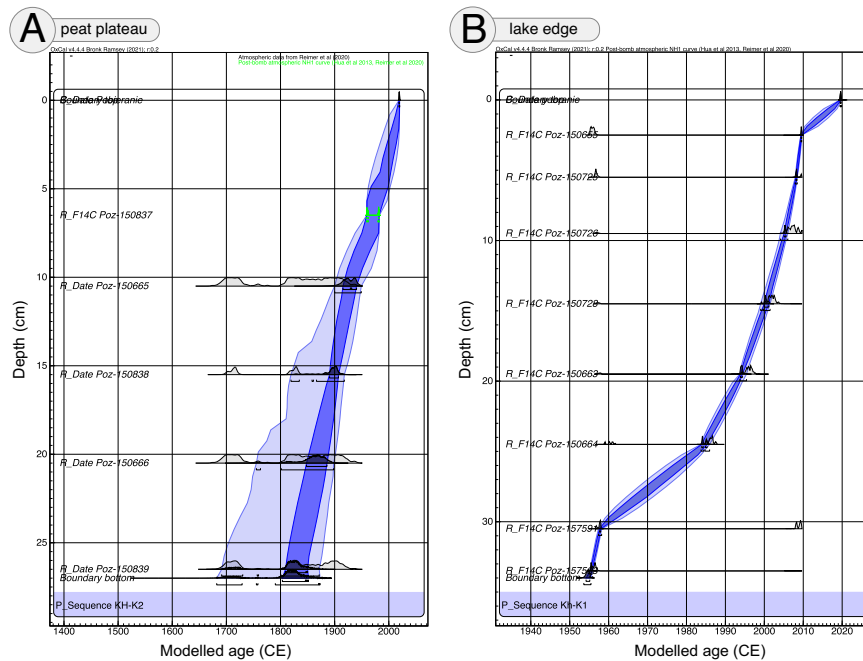


Figure 2 Age-depth models based on C¹⁴ dating for peat cores: A) Kh-K2 – peat plateau and B) Kh-K1 – lake edge. The dark and light blue areas provide the 68.3% and 95.4% confidence ranges of the model, respectively.

3.3. Testate amoebae analysis

Testate amoebae (TA) analysis was conducted following an established protocol (Booth et al., 2010). Sub-sampled material was shaken with distilled water and sieved through a 300 µm mesh. The material was examined using a light microscope at 200-400× magnification. For each sample, a minimum of 150 individual tests were counted and identified based on the available identification guides (e.g., Charman et al., 2000; Siemensma, 2022; Todorov and Bankov, 2019). The results of testate amoebae analysis were used for the quantitative depth to water table (DWT) and pH reconstructions.

3.4. Pollen, non-pollen palynomorphs (NPPs), and microcharcoal analysis

Pollen analysis was prepared following the standard procedure (Berglund and Ralska-Jasiewiczowa, 1986). To estimate the concentration of palynomorphs, *Lycopodium* markers were used (Stockmarr, 1971). For taxonomical identification, pollen keys (Beug, 2004; Faegri et al., 1989; Moore et al., 1994) and reference photographic collections were used. For each sample, at least 300-500 pollen grains of terrestrial plants were counted. The sum AP+NAP (arboreal and non-arboreal pollen) was calculated, excluding telmatic and aquatic taxa, spores, and non-pollen palynomorphs (NPPs). Microscopic charcoal particles (10-100 µm) and NPPs were counted during the analysis from the same slides. NPPs identification was based on Van Geel (2001) and Shumilovskikh et al. (2015). To determine regional fire activity, microcharcoal accumulation influx (MIC influx, particles·cm⁻²·yr⁻¹) was calculated by dividing the microcharcoal concentration (particles·cm⁻³) by peat accumulation rate (cm·yr⁻¹).

3.5. Plant macrofossil analysis

Samples were washed and sieved with distilled water using 125 µm mesh. To estimate the percentage volume of mosses and vascular plants, samples were examined with a stereoscopic microscope. The macrofossils were identified using various identification guides (e.g., Katz et al., 1977; Mauquoy and Geel, 2007; Tobolski, 2000). The subfossil vegetative fragments and carpological remains were counted but excluded from volume percentages and noted as present or absent in each sample.

3.6. Macrocharcoal analysis

Macroscopic charcoal (particles $\geq 100 \mu\text{m}$) analysis was used to conduct paleo fire reconstruction. All samples were bleached for 24 hours (Mooney and Radford, 2001) and then wet-sieved through $100 \mu\text{m}$ and $500 \mu\text{m}$ meshes. Macrocharcoal particles were counted with a stereoscopic microscope and divided into two groups: $100\text{-}500$ and $>500 \mu\text{m}$ to provide information about potential fire distance from the studied area (e.g., Conedera et al., 2009). To determine local fire activity, macrocharcoal accumulation influx (MAC influx, $\text{particles}\cdot\text{cm}^{-2}\cdot\text{yr}^{-1}$) was calculated by dividing the macrocharcoal concentration ($\text{particles}\cdot\text{cm}^{-3}$) by peat accumulation rate ($\text{cm}\cdot\text{yr}^{-1}$).

3.7. Organic matter content and C content

The content of organic matter (OM, %) was determined by loss on ignition (LOI) analysis following standard protocol (Heiri et al., 2001). Samples were oven-dried at 105°C for 12 h and then burned in a muffle furnace at 550°C for 3 h. To estimate dry bulk density (BD, $\text{g}\cdot\text{cm}^{-3}$), the weight of the sample after drying was divided by the fresh sample volume. The organic matter content was calculated as the difference between dry and burned sample weight, divided by dry sample weight (Chambers et al., 2011). The carbon content (g) was converted from the OM by assuming that organic C is $\sim 50\%$ of OM by mass (Chambers et al., 2011; Treat et al., 2016). The carbon accumulation rate (CAR, $\text{g C}\cdot\text{m}^{-2}\cdot\text{yr}^{-1}$) was calculated following equation (Tolonen and Turunen, 1996):

$$\text{CAR} = \frac{\text{PAR}}{1000} \times \text{BD} \times \text{C} \quad (1)$$

Where: CAR – carbon accumulation rate ($\text{g} \cdot \text{m}^{-2} \cdot \text{yr}^{-1}$), PAR – peat accumulation rate ($\text{mm} \cdot \text{yr}^{-1}$), BD – dry bulk density ($\text{g} \cdot \text{m}^{-3}$), C = C content ($\text{g C} \cdot \text{g}^{-1}$ dry weight)

3.8. Numerical analysis

All stratigraphic diagrams were plotted with Tilia graph software v3.0.1 (Grimm, 1991) and Grapher™ Golden Software. Peatlands' development stages were determined based on changes in TA community structure and related depth to water table (DWT) fluctuations. Zonation was based on CONISS using a *rioja* package in R (Juggins, 2020). The Shannon Diversity index was calculated for each TA sample using a *vegan* package (Oksanen et al., 2022) in R software (R Core Team, 2022). To understand the response of TA communities to past ecosystem disruptions, five TA functional traits were selected: mixotrophy, aperture size and position, shell compression, and biovolume. Based on TA functional traits, the community-level weighted means of trait values (CWM) was calculated for each community and each standardized trait to estimate their functional composition using the *FD* package (Laliberté et al., 2014) and TA functional traits established by Fournier et al. (2015). TA were also divided into four categories based on shell type: organic, organic-coated idiosomic, idiosomic, and agglutinated (Mitchell et al., 2008).

The Non-metric Multidimensional Scaling (NMDS) was applied to the TA species composition data from the Kh-K1 core using a *scikit-learn* library (Pedregosa et al., 2011) to detect temporal changes in community structure. Before the NMDS, the data were standardised using z-score standardization. The NMDS algorithm was set to use Euclidean distance and two dimensions. The K-Means clustering was applied to the transformed data and visualised with 95% confidence interval ellipses. The optimal number of clusters that maximized the Silhouette Score was selected as the optimal clustering solution (Fig. S1). Data visualization was carried out using a *matplotlib* (Hunter, 2007) and *seaborn* (Waskom, 2021) libraries. Calculations were conducted using Python in a Google Colaboratory (Google Colab) environment. The NMDS was performed only on core Kh-K1, as this core captures the most dynamic ecological transitions, and CONISS was considered sufficient for summarizing patterns in Kh-K2.

235 To reconstruct changes in DWT, Khanymei transfer function for discontinuous permafrost peatlands was applied (Halaš et al., 2023), and pH changes were reconstructed using Asian transfer function (Qin et al., 2021). Reconstructions were carried out using the C2 program, version 1.8.0. (Juggins, 2007).

4. Results

240 This section presents the outcomes of the multi-proxy analyses of two peat cores, Kh-K1 (lake edge) and Kh-K2 (peat plateau). The results are organized according to stratigraphic zones identified based on changes in testate amoeba (TA) community structure and associated fluctuations in depth to water table (DWT). For the peat core Kh-K1, four zones (Kh1-A to Kh1-D) were distinguished, and for Kh-K2, six zones (Kh2-A to Kh2-F). These zones provide a framework for describing and interpreting past hydrological and ecological dynamics (Fig. 3, 5, 6).

4.1. Kh-K2 - peat plateau

4.1.1. Zone Kh2-A (ca. 1814-1832 CE)

245 In the first zone Kh2-A there is a dominance of Unknown TA_Khan (Fig. 4), *Diffflugia pulex* type, and the presence of *Centropyxis aculeata* type (Fig. 3A) – indicators of wet conditions (Halaš et al., 2023). Bigger TA aperture size, higher shell biovolumes, and more spherical shells also suggest wet conditions. TA species with agglutinated shells are the most abundant in this zone. Based on TA, this zone was characterized by wet conditions, with DWT around 4 cm and a pH of 5.1. The presence of green algae genera *Botryococcus* (Fig. 5A) also indicates a wetter environment (Pandey et al., 2023), while the presence of fungi *Helicoon pluriseptatum* HdV-30 a shift towards drier oligotrophic conditions (Kuhry, 1997). This period is
250 characterized by a ligneous layer with roots and wood (Fig. 5A); however, ca. 1830 CE *Sphagnum* Secc. *Cuspidata* starts to take over the peatland surface. Numerous seeds of shrubs (*Vaccinium* sp.) and sedges (*Carex* sp.), as well as leaves of dwarf shrubs (*Betula nana*), are present in the sediment. In this zone, a high peak of *Betula* pollen was recorded, as well as the presence of shrubs *Rhododendron tomentosum*, Ericaceae, and *Vaccinium*. After ca. 1820 CE, a decrease in *Betula* pollen was inferred, which coincides with the period of high MIC that occurred between 1814 and 1835 CE (Fig. 5A, 6A). Peat
255 accumulation in this period remains low and stable (~1.3 mm/yr), while carbon accumulation decreases from 29.5 g/m²/yr to 8.8 g/m²/yr.

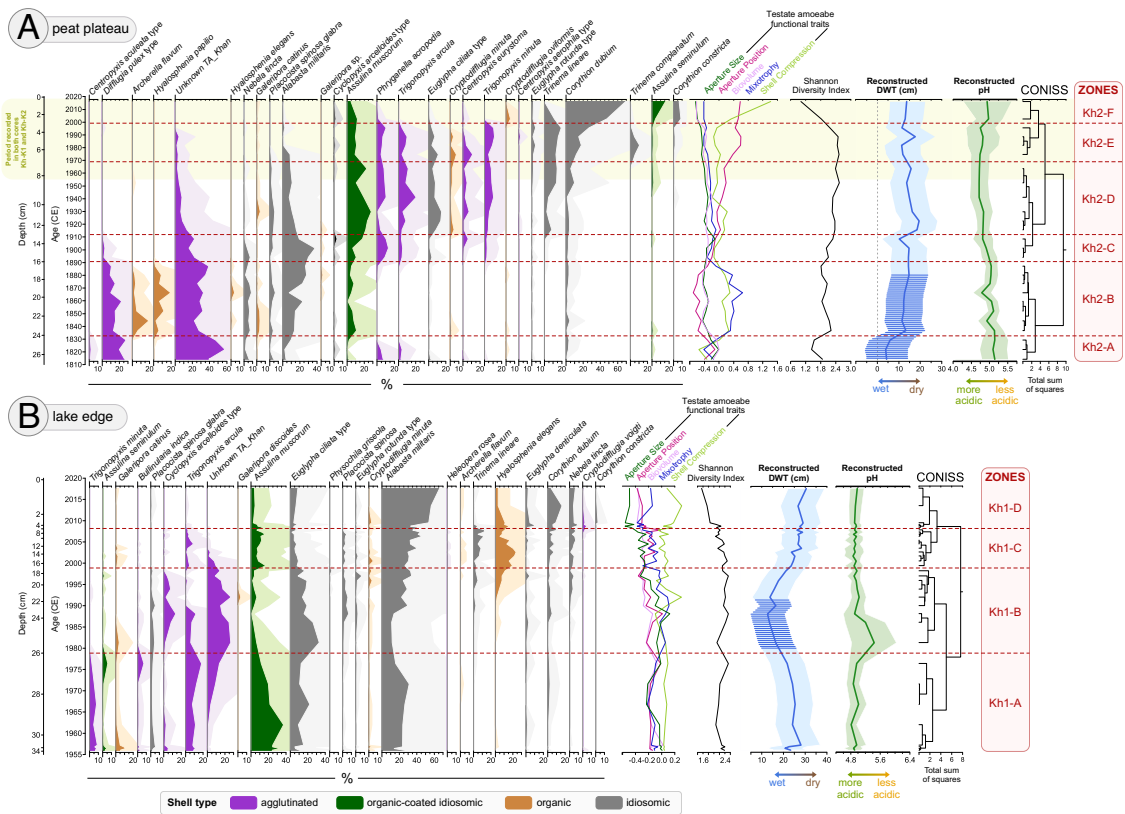


Figure 3 Testate amoebae (TA) diagram (abundance >3%) with 5× exaggeration for peat cores: A) Kh-K2 – peat plateau and B) Kh-K1 – lake edge. TA species are grouped by shell type, as indicated by the colour legend below the plot. The diagram includes community-weighted TA functional traits, Shannon Diversity index, reconstructed depth to water table (DWT) based on Halaš et al. (2023), and reconstructed pH based on Qin et al. (2021). Shaded areas for DWT and pH represent bootstrap reconstruction errors. The hatching on the DWT indicates a reconstruction potentially affected by error due to the presence of >25% of a new TA species. Species are sorted by weighted average (WA). Zonation was based on testate amoebae CONISS.

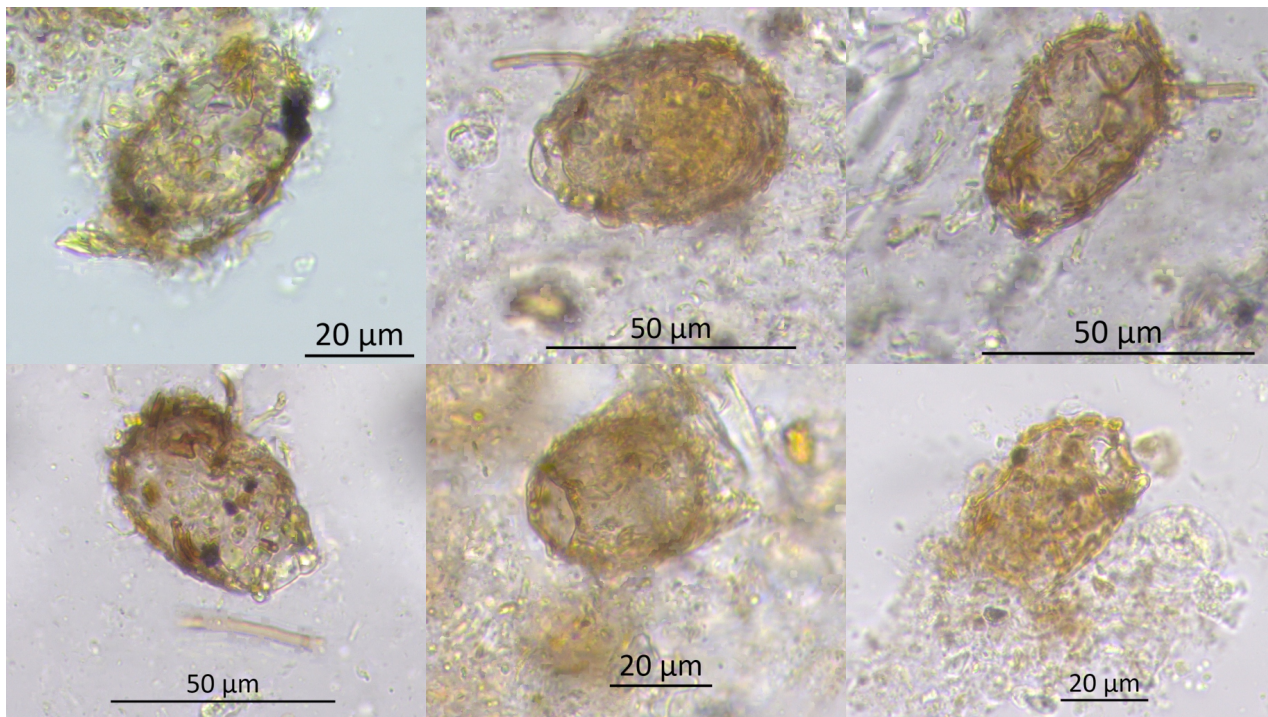


Figure 4 Light microscope images of an unidentified testate amoeba (Unknown TA_Khan) found in samples from Khanymei peatland. The taxon exhibits an ampulla-shaped test with a distinct collar or neck. The aperture is circular, and larger mineral particles are visible inside. Further taxonomic identification is needed.

4.1.2. Zone Kh2-B (ca. 1832-1890 CE)

270 In zone Kh2-B there is a disappearance of *Centropyxis aculeata* type and a decrease of *Diffflugia pulex* type – wet indicators (Fig. 3A). Intermediate indicators such as Unknown TA_Khan, *Archerella flavum*, and *Hyalosphenia papilio* appear, and dry indicators are more abundant (e.g., *Alabasta militaris*, *Assulina muscorum*) (Bobrov et al., 1999; Halaš et al., 2023). The functional traits of TA change, shells become more compressed with smaller biovolume and smaller aperture in more

275 moisture conditions and low pH in *Sphagnum* (Lamentowicz et al., 2020), are the most abundant in this zone. In this zone DWT increases and stabilises between 12-15 cm, while peatland acidification continues (pH = 5.0) with periods of lower pH values (pH = 4.8). *Sphagnum* Secc. *Cuspidata* is a dominant peatland vegetation between 1835 and 1895 CE (Fig. 5A). HdV-83 associated with wet phases of *Sphagnum* becomes present after ca. 1845 CE (Shumilovskikh et al., 2015). NPP indicators of very wet conditions (HdV-30) and green algae *Botryococcus* decline after 1860 CE. We inferred the return of *Pinus* in

280 pollen, which becomes similarly abundant as *Betula*. After 1865 CE, a decrease in shrubs (e.g. *Ericaceae*, *Vaccinium*) and an increase in herbs (e.g. *Rubus chamaemorus*) was inferred. Leaves and seeds of shrubs (e.g., *Betula nana*) and sedges (*Carex* sp.) are very abundant in this zone. This zone has a stable peat accumulation rate (~1.4 mm/yr) and high content of organic matter (~98.3%) (Fig. 6A). Carbon accumulation rate oscillates between 4.3 and 9.2 g/m²/yr. Low MIC values indicate low regional fire activity; however, higher MAC (>500 µm) values ca. 1890-1900 CE indicate a period of very local fires.

285

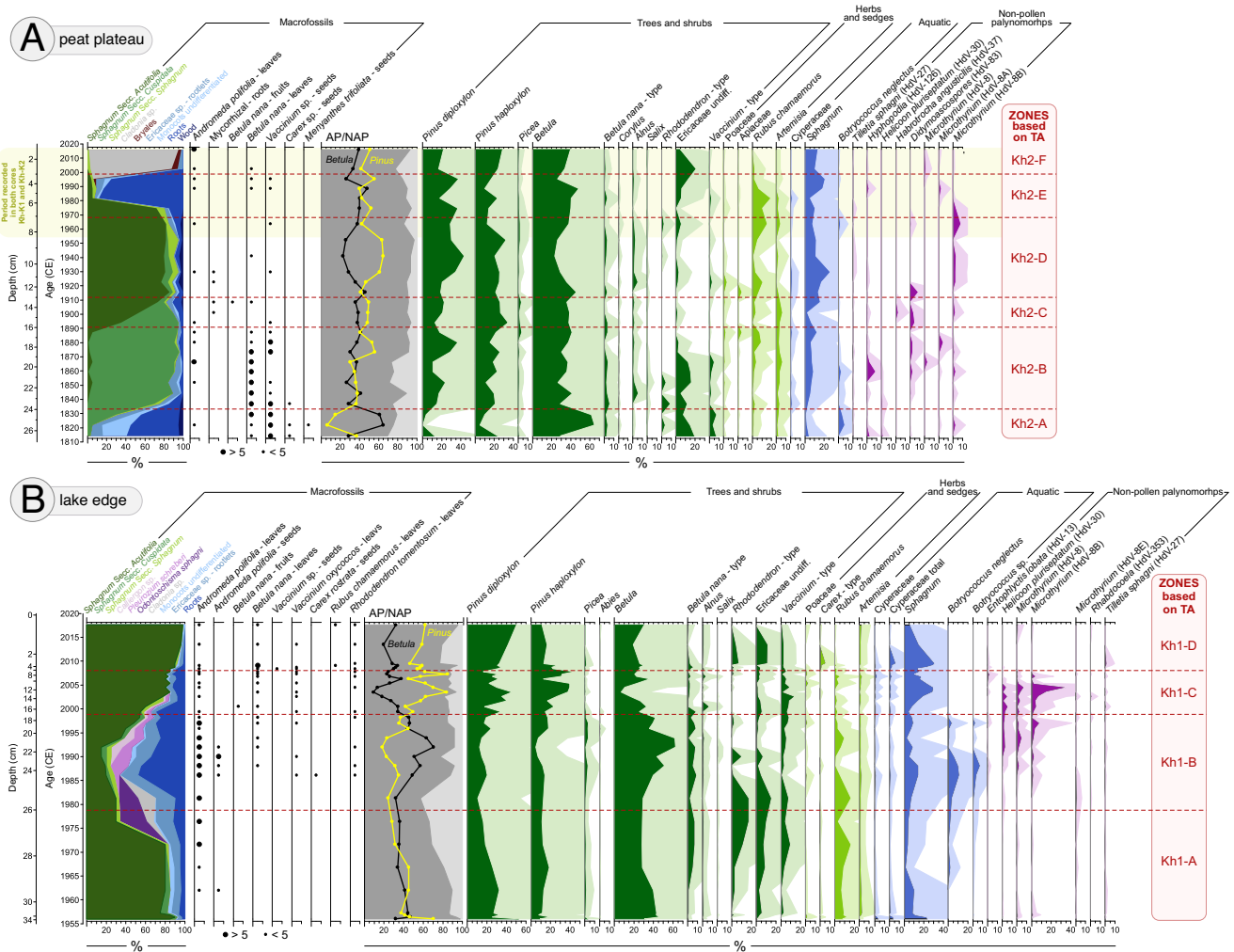


Figure 5 Macrofossils and pollen diagram with 5× exaggeration from peat cores: A) Kh-K2 – peat plateau and B) Kh-K1 – lake edge. The subfossil vegetative fragments and carpological remains are represented as either present or absent in each sample. Zonation based on testate amoebae CONISS was added to the graph.

Zone Kh2-C was a 20-year transitional phase when a significant shift in TA community structure was inferred, and dry indicators like *Alabasta militaris* and *Assulina muscorum* become dominant (Bobrov et al., 1999) (Fig. 3A). There is also an increase in *Cyclopyxis arcelloides* type and *Phryganella acropodia*, which tolerate wetter conditions (Halaš et al., 2023). More species with larger apertures appear, while mixotrophic TA and species with organic shells almost disappear. Based on TA reconstruction, this zone was characterised by a short-term decrease in DWT to 10 cm ca. 1910 CE. The presence of rotifer *Habrotrocha angusticollis* (HdV-37) (Fig. 5A) also indicate periodic wetting (Shumilovskikh et al., 2021). A gradual transition in *Sphagnum* species from *Sphagnum* Secc. *Cuspidata* to *Sphagnum* Secc. *Acutifolia*, typically a hummock group of species (Fig. 5A) (Malmer, 1988), was inferred together with a decrease in reconstructed pH (<5). Leaves and seeds of shrubs and sedges become almost absent in the sediment after 1865 CE. Peat characteristics remain stable with no significant change in peat accumulation and organic matter content (Fig. 6A). Initially 11.9 g/m²/yr, the carbon accumulation rate decreases to 4.7 g/m²/yr as DWT drops. An increase in MIC was inferred, which indicates higher regional fire activity.

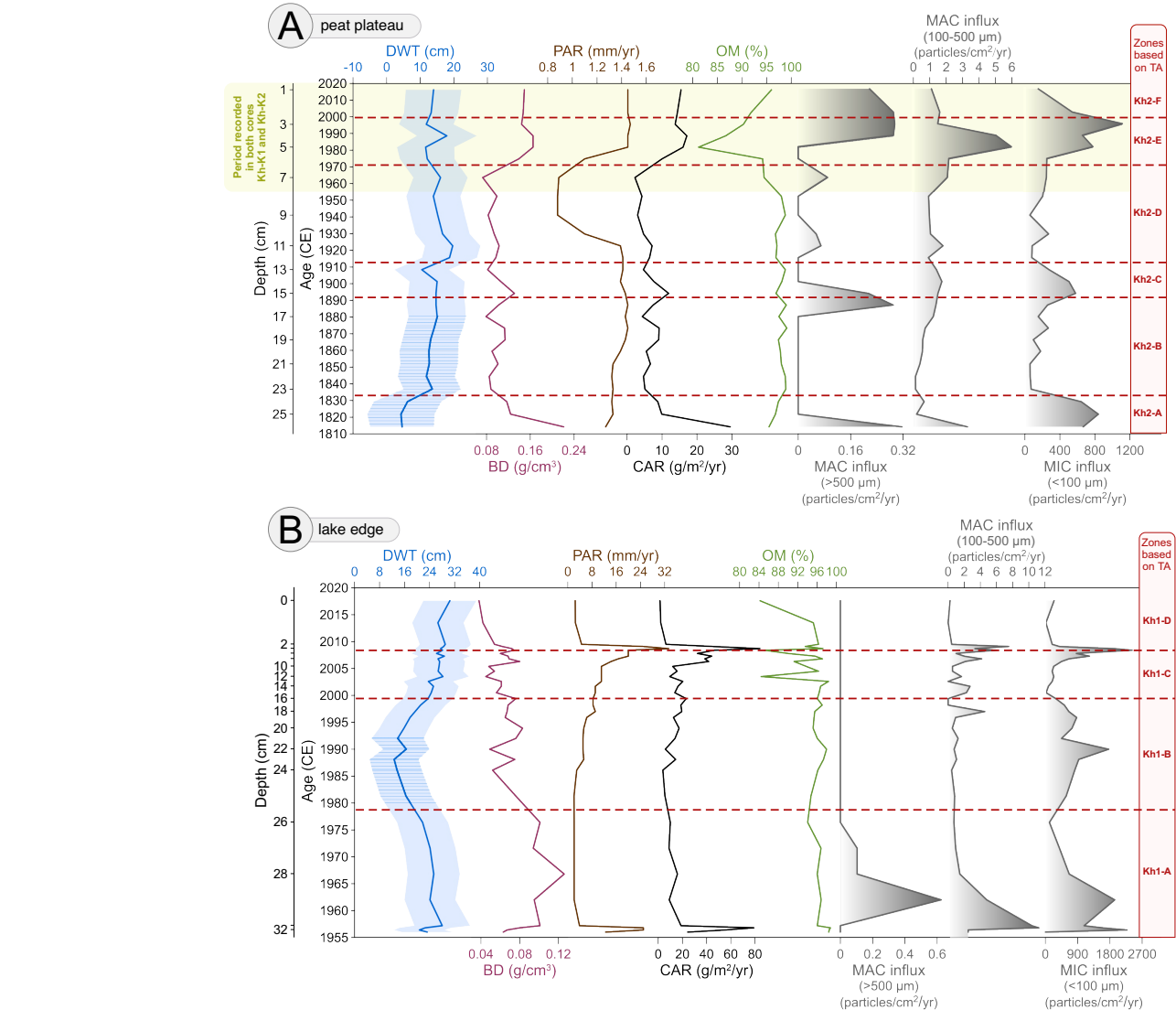


Figure 6 Changes in depth to water table (DWT) with bootstrap reconstruction errors (lighter blue), bulk density (BD), peat accumulation rate (PAR), carbon accumulation rate (CAR), organic matter content (OM), macrocharcoal influx >500 μm and 100-500 μm (MAC), and microcharcoal influx < 100 μm (MIC) in peat cores A) Kh-K2 – peat plateau and B) Kh-K1 – lake edge. Zonation based on testate amoebae CONISS was added to the graph. The hatching on the DWT indicates a reconstruction potentially affected by error due to the presence of >25% of a new TA species.

4.1.4. Zone Kh2-D (ca. 1910-1970 CE)

In zone Kh2-D, *Diffflugia pulex* type disappears, and the abundance of Unknown TA_Khan declines to below 10% (Fig. 3A). At the same time, dry indicators, like *Cryptodiffugia minuta*, *Assulina muscorum*, or *Trigonopyxis arcuata* appear in higher abundance (Bobrov et al., 1999). More species with idiosomic and organic-coated idiosomic shells appear. Taxa with smaller aperture sizes with cryptic positions become dominant (Fournier et al., 2015). At the beginning of this zone DWT significantly increases to 19.7 cm and later oscillates ~15 cm. Acidification progresses reaching the lowest pH values in the record (pH = 4.7). This zone is dominated by *Sphagnum* Secc. *Acutifolia* (80%) with some addition of *Sphagnum* Secc. *Sphagnum* (Fig. 5A). Less shrub remains were inferred; however, dead wood became more present in the sediment. Fungal fruit bodies of *Microthyrium* HdV-8B are more abundant, which has been associated with drier or more oligotrophic conditions (De Klerk et al., 2009). We inferred a lower frequency of shrubs and an increasing presence of herb *Rubus chamaemorus*. Between 1930 and 1960 CE, *Pinus pollen* is more abundant than *Betula* pollen. This coincides with a period of lower peat (~0.9 mm/yr) and carbon accumulation 2.2-7.2 g/m²/yr (Fig. 6A). The low values of MIC and MAC indicate a period of low local and regional fire activity.

4.1.5. Zone Kh2-E (ca. 1970-2000 CE)

In this zone, similar TA species are present as in the previous one but with a lower abundance of Unknown TA_Khan, *Assulina muscorum*, and *Alabasta militaris* (Fig. 3A). Species with drier moisture preferences like *Trinema lineare* or *Corythion dubium* appear more frequently (Bobrov et al., 1999). Functional traits adapting species to drier conditions were inferred, such as smaller aperture size, biovolume, compressed shells, and more cryptic aperture. Zone Kh2-E was characterized by fluctuating DWT, with an initial decrease to 12 cm and an increase to 18 cm by ca. 1990 CE. Acidification decreases slightly with high pH variability (reconstruction error 0.4 pH). We inferred a ligneous layer with >80% of roots/rootlets and decrease in *Sphagnum* species after 1980 CE (Fig. 5A). After a period of domination of *Pinus* pollen between 1920 and 1960 CE, in this zone, the share of *Betula* and *Pinus* pollen remain, at a similar level of ~35%. After 1990 CE, the shrub Ericaceae becomes more frequent while herbs *Rubus chamaemorus* and *Artemisia* almost disappear. Between 1975 and 2000 CE, high MIC and MAC values (high local and regional fire activity) and a decrease in organic matter content to 81% were inferred (Fig. 6A). Peat and carbon accumulation increase to 1.4 mm/yr and 17.1 g/m²/yr, respectively.

4.1.6. Zone Kh2-F (ca. 2000-2019 CE)

In the last zone Kh2-F, the Shannon Diversity Index indicates low diversity in the TA community structure, which from 2000 CE is dominated by *Corythion dubium* (>50%) (Fig. 3A). The dominance of TA with idiosomic shells and the disappearance of species with agglutinated shells were inferred. TA shells become strongly compressed with small biovolumes and cryptic apertures. Reconstructed DWT is stable ~14 cm, and pH increases to 4.9 but with high model error (0.65). Surface vegetation consists mainly of *Cladonia* lichens (>85%), which appeared on peatland ca. 2000 CE (Fig. 5A). A peak in Ericaceae abundance was inferred, while other shrubs are absent. The low values of MIC indicate a decrease in regional fire activity; however, we found more MAC (>500 µm) particles in the sediment, which indicate that fire was present very locally (Fig. 6A). Organic matter content increases to 96% and carbon accumulation to ~15 g/m²/yr. Lichen and other moss accumulation rate is 1.4 mm/yr.

4.2. Kh-K1 – lake edge (destabilised peat plateau margin)

4.2.1. Kh1-A (ca. 1955-1979 CE)

In the first zone Kh1-A, dry species *Alabasta militaris* and *Assulina muscorum* dominate at the beginning of the record (Bobrov et al., 1999). The abundance of *Assulina muscorum* subsequently decreases, while Unknown TA_Khan

increases until 1979 CE. TA species with organic-coated idiosomic shells are highly abundant throughout the zone. Wet conditions were inferred at the beginning of the zone, followed by a rapid increase in DWT to 28 cm, which then slowly decreases to 17 cm by 1979 CE (Fig. 3B). The reconstructed pH indicates acidic conditions (pH = 4.8), with a slight increase in pH to 5.0 by 1979 CE. Local vegetation is dominated by *Sphagnum* Secc. *Acutifolia* with some addition of roots, rootlets, and monocots until ca. 1972 CE (Fig. 5B). As the DWT decreases liverworts *Odontoschisma sphagni* commonly found on *Sphagnum* hummocks/mounds but also on wet peat, appears (Blockeel et al., 2014), as well as lichens *Cladonia* sp. Both are present in the sediment between 1972 and 1986 CE. Shrubs pollen, particularly *Rhododendron*-type, and dwarf shrubs *Betula nana* increase after 1960 CE. An increase in abundance of green algae *Botryococcus*, which indicates wetter conditions was inferred after ca. 1965 CE (Pandey et al., 2023). Peat and carbon accumulation is high initially (12.5-25 mm/yr and 24.4-79.0 g/m²/yr respectively); however, as DWT increases after 1957 CE it slows down (2.1 mm/yr and 10 g/m²/yr) (Fig. 6B). This zone is characterized by high MIC and MAC values until ca. 1965 CE, which indicates high local and regional fire activity.

4.2.2. Zone Kh1-B (ca. 1979-1999 CE)

In this zone, the structure of TA community changes (Fig. 7, 3B), TA species with agglutinated shells Unknown TA_Khan and *Cyclopyxis arcelloides* type, indicators of intermediate or relatively wet conditions, peak in abundance (Halaš et al., 2023; Warner and Charman, 1994). At the beginning of the zone *Euglypha ciliata* type is very abundant. *Galeripora discoides*, associated with rapid water table fluctuations (Lamentowicz et al., 2009), is present between 1992 and 1995 CE. After 1992 CE *Hyalosphenia elegans*, *Alabasta militaris*, and *Nebela tinctoria* start to appear more frequently in the record. TA shells become more compressed, and aperture size increases. Some mixotrophic species (e.g., *Placocista spinosa*) appear, which may indicate stable conditions, but heterotrophic species are still dominant. This zone is characterised by an initial decrease in DWT from 17 to 12 cm by 1988 CE, followed by a gradual increase, reaching 24 cm by 1999 CE. Higher pH was inferred on the site between 1980 and 1992 CE, but when drying starts, pH falls below 5.0 again. The peat is dominated by roots and Ericaceae sp. rootlets (Fig. 5B). *Sphagnum* Secc. *Acutifolia* accounts for ~30% of plant macrofossils. When lichens are present, more non-arboreal taxa, especially shrubs, e.g., Ericaceae and herb *Rubus chamaemorus*, were inferred. Lichens and liverworts are replaced ca. 1985 CE by *Calliergon* sp. and *Pleurozium schreberi*, which grows on drier hummocks/mounds between wet *Sphagnum* (Street et al., 2013). More leaves and seeds of shrubs are found in the sediment after 1985 CE; however, the abundance of their pollen decreases. The most subfossil vegetative fragments belong to *Andromeda polifolia*, frequently found in low hummocks and lawns (Jacquemart, 1998). Abundance of green algae *Botryococcus* and *Sphagnum* spores starts to decline after ca. 1990 CE. Throughout the zone, a presence of fungi *Helicoon pluriseptatum* HdV-30, and fungal fruit bodies of *Microthyrium* HdV-8 and HdV-8B was inferred. Between 1980 and 1995 CE, *Betula* pollen is more abundant than *Pinus* pollen. The high MIC values indicate high regional fire activity, especially ca. 1990 CE (Fig. 6B). Organic matter content is high and stable ~96%. Peat and carbon accumulation is stable at the beginning of the zone but increases from 2.0 to 8.3 mm/yr and 3.8 to 23.1 g/m²/yr, respectively, between 1988 and 2000 CE.

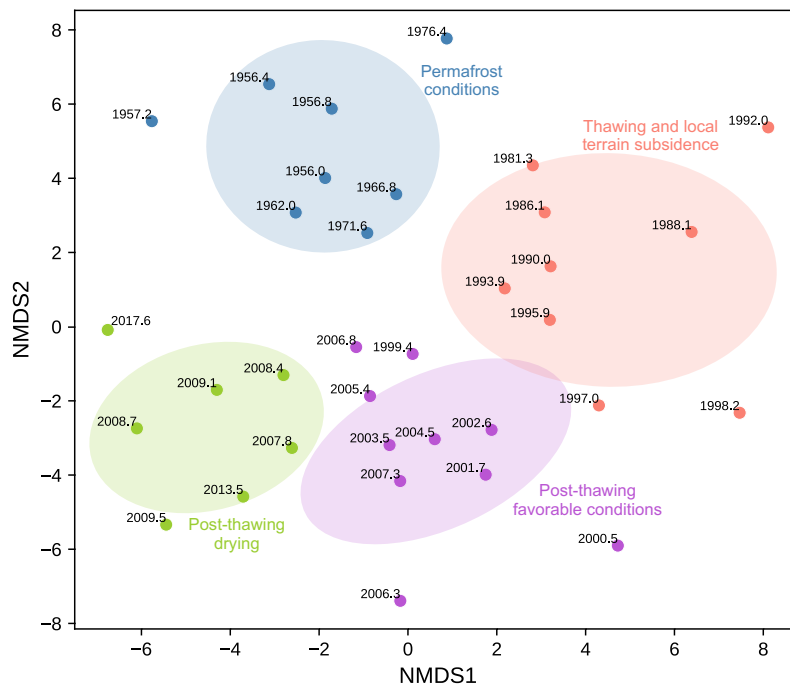


Figure 7 Two-dimensional NMDS ordination plot with K-Means clustering showing the distribution of testate amoebae samples from the Kh-K1 core (lake edge) over time. Ellipses represent the 95% confidence interval based on the covariance matrix of each cluster. Each point represents a sample, with year labels indicating temporal changes.

4.2.3. Kh1-C (ca. 1999-2008 CE)

In zone Kh1-C, the TA community structure changes again, with the most dominant species being *Alabasta militaris* (Fig. 3B, 7). We also inferred increased abundance of *Trigonopyxis arcula*, *Assulina muscorum*, and *Hyalosphenia elegans* in this period. Species with organic shells are more abundant, whilst agglutinated shells almost disappear. Characteristic of minerotrophic peatlands, *Heleopera rosea* is only present in this zone (Carballeira and Pontevedra-Pombal, 2021). The predominance of TA shells with smaller biovolume and aperture size with more cryptic position, indicate drier conditions. This zone is characterized by DWT ~26 cm and pH 4.9. After 2003 CE, *Sphagnum* Secc. *Acutifolia* once again becomes a dominant species whilst other plant species disappear (Fig. 5B). Roots and leaves of shrubs are still abundant. The expansion of *Pinus* pollen, disappearance of shrub *Rhododendron*-type, and low frequency of herbs were inferred. Around 2000 CE, green algae *Botryococcus* disappears from the sediment. We inferred an increase of *Sphagnum* spores, which coincides with a peak in fungal fruit bodies of *Microthyrium* HdV-8B and HdV-8. *Helicoon pluriseptatum* HdV-30, indicators of a transition from wetter to drier conditions (Shumilovskikh et al., 2021), declines after 2008 CE, as well as other fungi. Throughout this zone, peat accumulation increases from 9.1 to 20.0 mm/yr, with the peak in 2008 CE (Fig. 6B). Organic matter content is unstable and varies from 84.4 to 98.4% between 2002 and 2008 CE. Periods with lower content of organic matter coincide with peaks in MAC (local fire activity). Carbon accumulation increases from 13.7 to 44.2 g/m²/yr but decreases during periods when higher local fire activity was inferred.

4.2.4. Kh1-D (ca. 2008-2019 CE)

In the last zone, several TA species, e.g., *Cyclopyxis arcelloides* type and Unknown TA_Khan, disappear, while two new species *Cryptodiffugia voigti* (dry indicator) and *Corythion constricta* (intermediate) appear (Halaš et al., 2023) (Fig. 3B). The Shannon diversity index indicates a more homogeneous TA community structure dominated by *Alabasta militaris* (>50% of all shells). There is a dominance of TA species with smaller biovolume, more compressed shells, with smaller apertures, and idiosomic shells. In this zone the conditions are dry and stable with DWT ~28 cm and pH 4.9 (Fig. 3B). Surface vegetation is dominated by *Sphagnum* Secc. *Acutifolia* with some roots, Ericaceae sp. rootlets, and monocots (Fig. 5B). Leaves

of shrubs *Betula nana*, *Vaccinium oxycoccos*, and *Rhododendron tomentosum* are still present, and *Pinus* pollen still dominates over *Betula* pollen. A high abundance of *Sphagnum* spores was inferred. The beginning of the zone is characterized by high peat (20.0-33.3 mm/yr) and carbon accumulation (45.0-84.0 g/m²/yr) and high local and regional fire activity (high values of MIC and MAC) which significantly decrease after ca. 2009 CE (Fig. 6B). Following the intense fire period, peat and carbon accumulation slow down (2.5 mm/yr and 2.1 g/m²/yr, respectively). Pollen of shrubs and sedges is more abundant after 2009 CE (Fig. 5B). Organic matter content for the top layer decreased to 84.2%.

5. Discussion

5.1. Development of Western Siberian peatlands from the end of the Little Ice Age till modern times

Records from peat plateau core Kh-K2 show that at the beginning of the 19th century, the study site experienced wetter conditions with high carbon accumulation until ca. 1830 CE (Fig. 3A, 6A). On the Khanymei peatlands, this period was characterized by the presence of microalgae *Botryococcus*, typically found in fresh water wetlands (Pandey et al., 2023), which can also serve as an indicator of temporary water stagnation, as observed in Central European peatlands (Marcisz et al., 2015). Our results align with findings from more south-eastern sites obtained by Feurdean et al. (2022) and Willis et al. (2015), where between 1400 and 1850 CE, an increase in water level was inferred. These reconstructions overlap with the presence of the Little Ice Age (LIA, 1600-1850 CE) in the Northern Hemisphere (Mann, 2002). However, not all of the records from Western Siberia show the same trend; the LIA was a period of dry conditions on the southwest peatlands (Lamentowicz et al., 2015; Zakh et al., 2010). Although wetter conditions on a peatland usually limits fire activity (Nelson et al., 2021) on our site we inferred more local and regional fires (Fig. 6A). Higher fire activity and carbon accumulation at the end of LIA was also inferred on Plotnikovo Mire, where fires were associated with Russian exploration, which may also have affected the Khanymei region (Feurdean et al., 2019; Naumov, 2009).

After 1830 CE, the Khanymei site experienced drying, which resulted in the sudden disappearance of several TA species and increased acidification (Fig. 3A). The peatland was overtaken by *Sphagnum* Secc. *Cuspidata* and maintained a largely stable DWT till the end of the century (Fig. 3A). Period of drying (1830-1880 CE) overlaps with an increase in reconstructed mean June-July air temperature from tree rings in the Ob River valley (Gurskaya et al., 2012), and increased abundance of *Pinus* pollen. From 1885 CE, we inferred a transition of *Sphagnum* species from Secc. *Cuspidata* to *Acutifolia*, which indicate mound development (Malmer, 2014), this transition coincides with a decline of summer air temperature between 1880 and 1900 CE (Gurskaya et al., 2012) and follow a period of local fires (Fig. 6A). The post-fire recovery of *Sphagnum* Secc. *Acutifolia* was also observed on boreal peatlands in Western Canada (Kuosmanen et al., 2023) and Northern Europe (Sillasoo et al., 2011).

Different proxies like plant macrofossils, rhizopods, oribatid mites, diatoms, and testate amoebae have been tested as indicators of past environmental changes in permafrost peatlands (Lamarre et al., 2012; Markkula et al., 2018; Sannel and Kuhry, 2008; Wetterich et al., 2011). Markkula et al. (2018) demonstrated that some species of oribatid mites can be useful to detect past permafrost occurrence in peatlands; however, this proxy was not used in this study. Divergent plant succession trajectories in permafrost peatlands make it difficult to find a clear palaeoecological indicator of past aggradation (Treat et al., 2016). However, some studies suggest that the growth of *Sphagnum* Secc. *Acutifolia* in northern regions can precede permafrost aggradation (Pelletier et al., 2017; Sannel and Kuhry, 2009; Treat and Jones, 2018; Zoltai, 1993). This may indicate that on our site, permafrost started to aggrade ca. 1900 CE, taking advantage of the emergence of the denser and more insulating Secc. *Acutifolia* and periodic cooling in the summer months. Occurrence of *Sphagnum* Secc. *Acutifolia* and root/rootlet layers, which were considered by Sannel and Kuhry (2008) as indicators of permafrost conditions, can also serve as proof of permafrost presence on the study site after 1900 CE. However, because permafrost aggradation and degradation can co-occur

within the same peatland (Zoltai, 1993), details regarding permafrost existence on the study site may be considered as a local process that needs more sites to be better understood in space.

The turn of the 19th century has also been marked by regional fires (Fig. 6A). Unfortunately, limited high-resolution fire records from Western Siberia make it difficult to compare if this fire period appears in a larger area. However, the increased regional fire activity may be linked to the fact that between 1896 and 1914 CE, Siberia became Russia's principal region of colonization (Goryushkin, 1991). Fire was widely used by new settlers for the construction of new roads and villages and the clearing of forests (Goryushkin, 1991). During dry and warm continental summers, these fires may have occasionally escaped control, leading to the spread of wildfires, that consumed drier peatland areas dominated by shrubs. After the period of higher fire activity, the region experienced a decrease in the shrub pollen, particularly Ericaceae and *Vaccinium*, as well as reduction in subfossil remains of *Betula nana* and *Vaccinium* on the peatland. This decrease in shrubs coincided with an increase in herbaceous species, particularly *Rubus chamaemorus* (Fig. 5A).

The beginning of the 20th century started with ca. 10 cm increase in DWT and an increased abundance of *Pinus* pollen (Fig. 3A, 5A). It is notable to mention that during *Pinus* pollen dominance (1920-1960 CE) there was a sequential emergence of fire-adapted Diploxylon pine species, followed by Haploxylon species that are better adapted to abiotic stress (Singh et al., 2023). Higher abundance of *Pinus* with higher resilience to drier conditions (Wei et al., 2019) and lower peat accumulation (<1.4 mm/yr) may indicate the occurrence of a drier period in the Khanymei region. Although, the reduced peat accumulation may also be related to the presence of organic matter-decomposing fungi *Microthyrium* HdV-8B (Fig. 3A). Additionally, the period of increased presence of *Pinus* pollen coincides with the Early 20th Century Warming that started ca. 1910 CE and peaked in the 1940s, and could have contributed to the occurrence of drier conditions in the region (Bengtsson et al., 2004; Bokuchava and Semenov, 2021). However, the reconstruction of the DWT on peat plateau suggests that during this period, there was a gradual increase in moisture content (Fig. 3A). Potential explanations for the lower reconstructed DWT values on the peat plateau include the influence of low-lying permafrost, which creates different environmental conditions for testate amoebae - the microorganisms on which the reconstruction is based - compared to groundwater in non-permafrost peatlands (Zhang et al., 2017). In this context, the concept of a classic DWT level may not apply; rather, it reflects the specific moisture conditions of the mosses themselves. Notably, *Sphagnum* Sec. *Acutifolia*, which is present at the study site during that period, tends to grow in very dense patches, and its ability to maintain wet capitula through capillary water transport (Rydin and Jeglum, 2013) suggests that the reconstruction may not accurately represent commonly understood peatland ground water level (Baird and Low, 2022). On the other hand, higher air temperatures likely triggered permafrost thaw on the peat plateau, increasing peat moisture and ultimately leading to a decrease in the reconstructed DWT. As a result, reconstructing and interpreting water levels in permafrost peatlands requires caution due to the unique hydrological dynamics of these ecosystems.

Since 1970 CE, an increase in reconstructed summer mean air temperature in the Ob River valley and anomalies in surface annual temperature (SAT) in the Northern Hemisphere have been observed (Bokuchava and Semenov, 2021; Gurskaya et al., 2012). A warming climate also affects permafrost temperature, causing it to rise and leading to permafrost degradation, which can result in ground instability, altered hydrology, and changes in carbon dynamics (Streletskiy et al., 2015). Observations of permafrost temperature at 10 m in Nadym (260 km from Khanymei) showed increase of 1.3°C between 1972 and 2009 CE (Romanovsky et al., 2010). These changes impacted the peatland ecosystems in Khanymei, where the marginal part of the peat plateau collapsed around 1980 CE (Fig. 3B). Between 1985 and 1995 CE, increasing moisture was inferred at the site, followed by a rise in peat and carbon accumulation rates (Fig. 6B). Similar, but more intensive patterns of collapse, followed by renewed productivity and peat accumulation, have been described in the Abisko region of Sweden (Swindles et al., 2015).

Increased regional fire activity recorded after 1970 CE indicates an overlap between natural fires and the human settlement expansion in the Khanymei region related to the construction of railways and oil exploration (Vaguet, 2013). Fires connected with gas and oil exploration were inferred at a similar time at the Mukhrino mire in the southern part of Western

490 Siberia close to Khanty-Mansiysk (Lamentowicz et al., 2015). Excessive construction activity in the close vicinity of the study area (<15 km) may have also contributed to a decrease in organic matter content, caused by a large supply of dust around 1980 CE (Fig. 6A). Data from the peat core Kh-K1 (1955-2020 CE) with higher temporal resolution, identified two distinct periods of higher fire activity in the region after 1970: 1985-1995 CE and 2006-2009 CE (Fig. 6B). Lower regional fire activity in our records in the last decades coincides with a decrease in burned area observed in Western Siberia after 2010 CE (Zhu et al., 495 2021). However, Zhu et al. (2021) noted that between 2003 and 2020 CE, wildfire extent in Siberia has been expanding westward, which may suggest that as climate change progresses, Western Siberia might be more affected by wildfires in the near future.

Fire activity in the peatland surroundings probably influenced shrub abundance in the area. We recognised a decrease in shrub pollen after 1880 CE, coinciding with a slight increase in local fire activity that persisted until 2000 CE, when shrubs, particularly Ericaceae, began to return (Fig. 5A, 6A). Data from core Kh-K1 provide more detailed insights, showing that shrubs became more abundant after 1965 CE. However, increased local fires between 1990 and 2010 CE once again led to a decline in shrub presence, followed by their reappearance after 2010 CE (Fig. 5B, 6B). Although shrubification is more commonly discussed in the context of the Arctic tundra (Buttler et al., 2023; Mekonnen et al., 2021), Forbes et al. (2010) recorded the effect of warming on shrub rings in the northwest Russian Arctic, with correlations extending over long distances 500 into the taiga zone of Western Siberia. Their findings revealed a clear *greening* trend at a regional scale from 1981 to 2005 CE, aligning with studies that have attributed a strong shrub component to the greening signal since 1980 CE. A similar signal is visible in our study site; however, it appears approximately 20 years earlier.

Increased air temperatures and higher fire activity in the past decades have impacted permafrost in Siberia, which remains in equilibrium with changing climate, continuous to alter peatland surface (Shur and Jorgenson, 2007). As permafrost 510 gradually degrades, the height difference between the peat plateau and depression increases, exposing the peat plateau to environmental influences. A similar process occurs when ice aggrades within the peat, causing the bog surface to uplift (Thibault and Payette, 2009). This creates drier conditions at the uplifted peatland surface, leading to the replacement of *Sphagnum* mosses with lichens (Seppälä, 1988; Thibault and Payette, 2009), which happened on the study site ca. 2000 CE (Fig. 5A).

515 5.2. Patterns of progressive permafrost thawing

Permafrost peatlands underwent significant but divergent hydrological changes in recent decades due to rising air temperatures and related permafrost thaw (Olefeldt et al., 2021; Zhang et al., 2022). In Khanymei permafrost peatlands, thaw-related surface transformation triggered changes in various elements of the ecosystem. Paleoreconstructions from peat cores Kh-K1 and Kh-K2 that cover the period from 1955 CE allowed the reconstruction of biological responses of peatland's 520 microhabitats and the creation of patterns of progressive permafrost thawing in a discontinuous permafrost zone (Fig. 8).

In the first stage, before thawing ca. 1979 CE, the peat plateau was characterized by dry conditions and lichen coverage (Fig. 8A). The presence of lichens temporarily constrains moss growth on peat plateau (Harris et al., 2018), which resulted in lower peat and carbon accumulation rates (Fig. 5A). Lichens are commonly found on mature peat mounds and palsas (Railton and Sparling, 1973), but their relatively low albedo reduces evapotranspiration, which can negatively affect ground cooling 525 during the summer (Rönkkö and Seppälä, 2003). The underlying porous peat typically serves as an insulator for permafrost; however, thawing and melting water are strongly absorbed by the peat, and with limited evapotranspiration, this leads to a decreased insulating effect and the deepening of the active layer. With higher air temperatures and the occurrence of fires, these changes accelerate permafrost degradation, leading to further thawing and surface transformation (Biskaborn et al., 2019; Hantemirov et al., 2022; Romanovsky et al., 2010).

530 As thawing began after 1979 CE, the deepening of the active layer released water, which, due to limited drainage, accumulated in low-lying parts of the peat plateau, leading to terrain subsidence and local inundation (Fig. 8B). A simulation

of ground subsidence run by Ekici et al. (2019) showed that between 2000-2010 some parts of Western Siberia experienced land subsidence of up to 0.7 m. This process has also been widely observed in permafrost areas in Canada (O'Neill et al., 2023; Wang et al., 2023). The higher moisture of subsided areas contributes to the submergence of lichens and their overgrowth by *Sphagnum* mosses. Wetter conditions also change the structure of TA communities to be dominated by wet (*C. arcelloides* type) and intermediate species (Unknown TA_Khan) and cause the emergence of various species of microalgae *Botryococcus* (Fig. 3B, 5B, 7).

Characteristic of this stage is the presence of new unidentified TA taxa (Unknown TA_Khan) (Fig. 4), which has an ampulla-shaped test with larger mineral particles, previously found in modern samples from Khanymei peatland and classified by Halaš et al. (2023) as *Diffflugia lucida* type. This taxon was rare in modern samples and mainly present in lichens with an optimum water level of ~9 cm, while in *Sphagnum* mosses mostly in wetter sites (~3 cm). The unknown taxa is an agglutinated xenosomic TA type that constructs its shells using grains and diatoms from its environment (Ogden and Hedley, 1980), with its presence significantly influenced by the water chemistry of its surroundings (Mitchell et al., 2000). Typical processes associated with permafrost thaw, such as soil subsidence, lichen submergence, and peat abrasion, impact the water chemistry in the region (Manasypov et al., 2017). Experiments conducted by Manasypov et al. (2017) indicate that submerged lichens and peat abrasion efficiently enrich lake water with soluble organic constituents and alter the chemical composition of thaw water, with lichens having the greatest impact. Therefore, we hypothesize that this specific water chemistry may influence the appearance of this taxa in the Khanymei peatland; however, further research is needed.

Water availability is considered one of the most critical factors of *Sphagnum* growth and decay, and therefore carbon accumulation (Bengtsson et al., 2016; Thompson and Waddington, 2008). Compared to the pre-thawing phase, rising water levels caused by thawing and terrain subsidence boosted peat and carbon accumulation on the lake edge (Fig. 6B, 8B). The shift from drier to wetter conditions may reduce fire severity (Nelson et al., 2021), as inferred in this study, as local fire activity decreases with slight wetting (Fig. 6B).

Further thawing significantly altered the peatland ecosystem structure (Fig. 8C). Further subsidence contributes to the formation of depressions filled with thaw water, creating small thermokarst lakes. Although there is an overall decline in the area of thermokarst lakes in discontinuous permafrost zones (Smith et al., 2005; Webb and Liljedahl, 2023), small lakes are still being formed (Polishchuk et al., 2015). Our data suggests that further thawing led to better drainage and accumulation of thawed water in the lake basin, causing drying of the lake edges. These contradict the typical dry plateau-wet hollow pattern and can be explained by the characteristics of the TA that were used in DWT reconstruction. TA is widely used to reconstruct DWT on peatlands (e.g., Charman et al., 2007); however, the primary control of species abundance is surface wetness (Woodland et al., 1998). Wetter conditions reconstructed on the peat plateau resulted from low-lying permafrost ~27 cm (Fig. 1D), which, during the thaw, increase peat moisture, influencing TA assemblages. Whereas on the lake edge, permafrost is absent, these assemblages are more vulnerable to *Sphagnum* surface drying, a process that is accelerated by increased evapotranspiration. Together with the drying of the peatland surface, we inferred an increase in local fire activity, similar to the pre-thawing period. Another important observation was that together with permafrost thawing we noted an increased abundance of several *Microthyrium* type fungal fruit bodies on the lake edge (type HdV-8 and HdV-8B) (Fig. 5B). In our study the highest abundance of HdV-8B fell in the period preceding the highest accumulation of peat and carbon but coincided with the greatest production of spores by *Sphagnum*. Given that fungi are involved in organic matter decomposition (Mitchell et al., 2003), this pattern may reflect a phase of active decomposition that preceded maximum peat accumulation. While we refrain from drawing firm conclusions, we consider this an intriguing signal that may warrant further investigation, particularly in light of the currently limited understanding of the ecological significance of these fungal remains.,

Many studies have indicated that global warming and permafrost thawing will convert high-latitude peatlands from a net atmospheric carbon sink to a source (Abbott et al., 2016; Harris et al., 2023; Schuur et al., 2015). However, this shift may not be linear due to the complexity of plant-microbial-soil interactions and the potential mitigation of carbon losses through

575 enhanced plant productivity (Berner et al., 2020; Epstein et al., 2013; Standen and Baltzer, 2021). In our study, increases in
peat and carbon accumulation were inferred in both the peat plateau and lake edge sites after thawing began ca. 1979 CE, with
the lake edge site being the most active in accumulation (Fig. 6, 8C). Although wetter conditions, considered better for
Sphagnum growth (Clymo, 1973), occurred in the subside area in the previous stage, increased peat accumulation was still
580 inferred even after the DWT increases. This suggests that thawing re-invigorated moss productivity by providing the necessary
moisture, allowing them to continue benefiting from the additional water supply even many years after the collapse (Swindles
et al., 2015). Vivid growth could also be explained by the dense structure of the dominant species of *Sphagnum* Secc. *Acutifolia*
that could still maintain a high rate of photosynthesis after DWT increases (Rydin and Jeglum, 2013). A higher abundance of
Sphagnum spores during this time confirms their robust potential for reproduction and colonization (Fenton and Bergeron,
2006). We hypothesize that the high values of peat and carbon accumulation inferred at the lake edge were a direct consequence
585 of beneficial conditions created by thawing in the previous stage. Our study suggests that these favourable conditions have
already happened on this part of the peatland, they were short-term and occurred in a limited area (Fig. 6B, 8C). However, it
is important to note that different stages of permafrost degradation can occur simultaneously within the region, as shown by
Swindles et al. (2015). Therefore, while our results are local, they highlight potential patterns of permafrost degradation and
associated environmental consequences that may arise at different times in the Khanymei region or other areas with
590 discontinuous permafrost in Western Siberia.

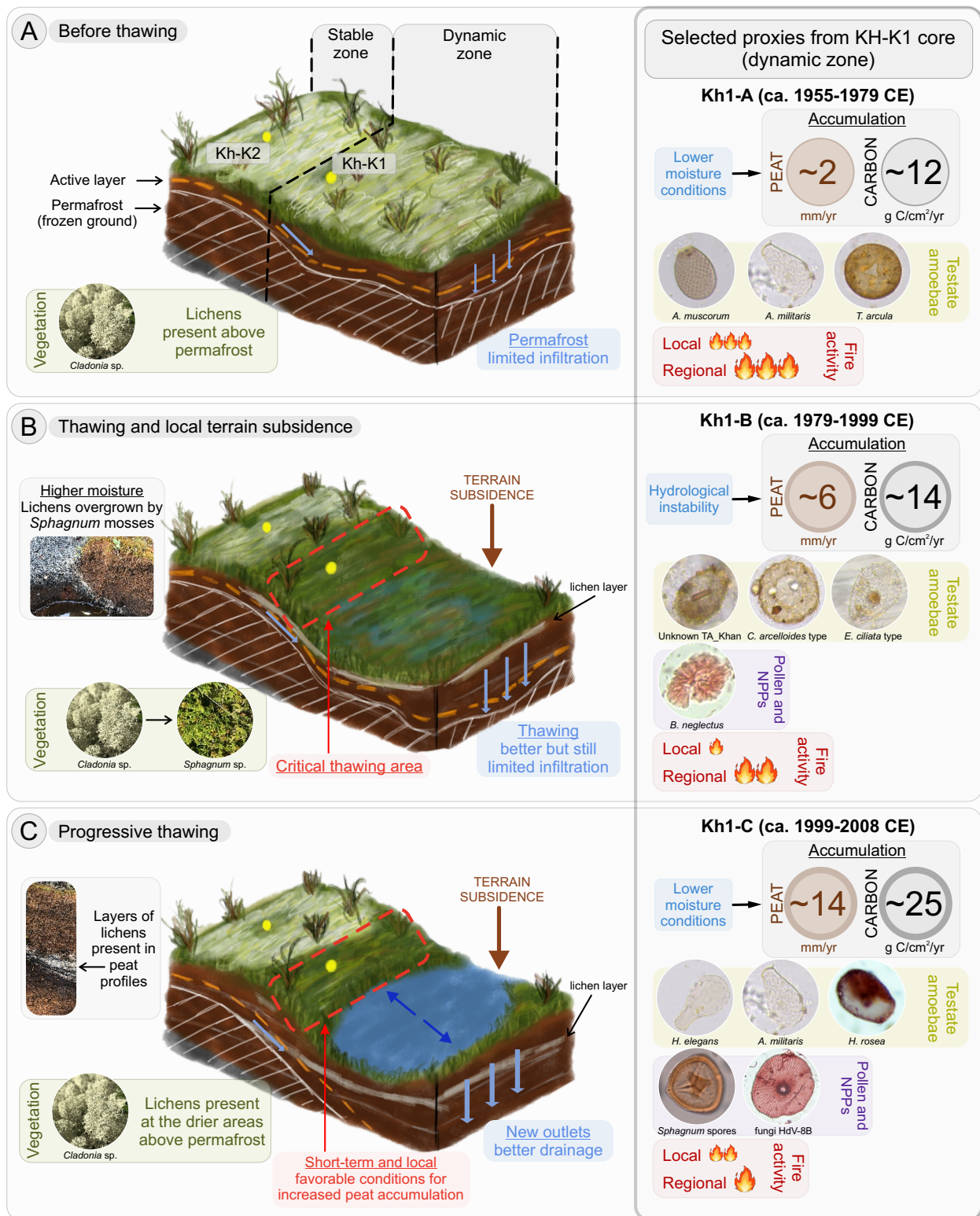


Figure 8 Illustration of stages of the progressive permafrost thawing in a discontinuous permafrost peatland based on cores Kh-K1 (lake edge) and Kh-K2 (peat plateau) with selected proxies. In the illustration, core Kh-K1 represents the dynamic zone, and core Kh-K2 represents the stable zone. The values for peat and carbon accumulation rates and intensity of fire activity shown in the right panel represent mean values from selected zones of core Kh-K1. Pictures of lichens, mosses, and peat profiles on the left panel come from the other peatlands in region to better present the process of lichen-*Sphagnum* shifts. Sources: photos of *Sphagnum* spores from Inglis et al. (2015).

5.3. Same mire – different perspective

The majority of palaeoecological reconstructions on peatlands are based on one or a few cores located in the same area to study local history (e.g., Lamentowicz et al., 2015; Novenko et al., 2023) or hundreds of kilometres to reconstruct regional history or trends (e.g., Feurdean et al., 2022; Willis et al., 2015; Zhang et al., 2022). In this study, we focused on the

differences between peat plateau-depression (lake edge, in this case) microhabitats. Our multi-proxy analysis showed that these microhabitats react differently, particularly in site-specific elements such as: peat and carbon accumulation, hydrology, plant macrofossil composition and occurrence of fungal NPPs (Fig. 3, 5, 6). The microhabitats described in our study are a characteristic feature of the landscape of discontinuous permafrost peatlands in Western Siberia. Our results show that peatland surface heterogeneity, especially in permafrost areas, leads to the occurrence of various simultaneous processes.

In non-permafrost regions, the typical hummock-hollow structure is in a certain state of equilibrium directly related to hydro-climatic conditions (Kulczyński, 1939; Rydin and Jeglum, 2013; Tobolski, 2000). Whereas in regions of discontinuous permafrost, palsa or peat plateaus/mounds are adjacent to the unfrozen peatlands or thermokarst lakes (Seppälä, 2011). The situation is specific because two very different environments are in close vicinity to each other. In this study, we distinguished two main zones within a short distance: stable and dynamic (Fig. 8).

The stable zone is characterized by the presence of permafrost in the ground, which creates stable conditions and an equilibrium on the peatland surface. In this zone, the water level was relatively stable or rising due to increase peat moisture from thawing. However, the processes occurring there were gradual and extended over time due to the presence of permafrost. In contrast, in the dynamic zone, thawing initially triggers cascading hydrological changes, consequently forcing habitat shifts (Fig. 3, 5, 6). These changes mostly occur in the lateral part of peat plateau, where data from the lake edge core (Kh-K1) allowed us to identify a critical thawing area (Fig. 8B). The described area is a part of the dynamic zone with the most noticeable and rapid changes due to its location between contrasting environments: a previously thawed and collapsed depression, and an ice-rich peat plateau (Fig. 8B). As a consequence of hydrological changes, expanding permafrost thawing leads to relatively rapid increase in DWT as a result of drainage towards the formed slough (Fig. 8C). However, only in this area a rapid but short-term improvement in hydrological conditions, with a simultaneous rapid increase in peat and carbon accumulation was reconstructed (Fig. 6B). This mechanism makes this area the most dynamic part of the peatland where permafrost thaw occurs.

The lateral part of the peat plateau (critical thawing area) where we inferred the most significant changes, although relatively small, has a significant impact on the permafrost core in the adjacent peat plateau. Post-thaw wetter peat conditions on the peat plateau margin allow higher heat penetration of the permafrost core (Railton and Sparling, 1973), accelerating its thaw and reducing plateau size. Currently, the shifting of this area and consequent increase in the area of drainless depressions and decrease in peat plateaus area is observed yearly, resembling a domino effect. These depressions eventually merge with adjacent ones to form larger lakes, which ultimately drain into a watercourse or river. Degradation of palsas and peat plateaus caused by lateral erosion and the formation of thermokarst lakes has also been observed in northern Norway, where since the 1950s, their total area has decreased by 33-71%, depending on the region (Borge et al., 2017).

It is important to emphasize that the high variability of permafrost peatlands requires careful interpretation of environmental records. Without a comprehensive approach, changes inferred in the peat profile might be misattributed to incorrect factors. Therefore, conducting multi-proxy analyses is essential to ensure accurate reconstruction of past and present environmental conditions in areas with current or past permafrost.

6. Conclusions

Our multi-proxy reconstruction provided new insights into the history of peatlands in the understudied region of Western Siberia. On Khanymei peatlands, the end of the Little Ice Age was marked by wetter conditions that predominated until 1840 CE. This period was followed by peatland drying and an increase in regional fire activity. Later peaks of increased regional fires correspond to key historical events, including the Russian colonization of Siberia at the beginning of the 20th century and intensified oil and gas exploration after 1970 CE. Plant indicators suggest that permafrost likely began to aggrade on the study site around 1900 CE. The presence of an ice core within the peat plateau limited moss growth, leading to low peat

and carbon accumulation. In recent decades, rising air temperatures have triggered permafrost thaw, transforming peatlands' ecosystem. Notably, the most dynamic changes occurred after 1979 CE, exhibiting considerable variation across different parts of the peatland. Our research highlights that permafrost thaw in the discontinuous permafrost zone in Western Siberia has driven significant but local transformations in peatland hydrology, vegetation, and microbial communities, with the lake edge being the most dynamic microhabitat. Thaw-related surface subsidence increased water availability, promoting *Sphagnum* growth and carbon accumulation, though these favourable conditions were short-term and limited to specific areas. Significant changes in testate amoebae communities and increased fungal activity indicate complex interactions between thaw dynamics and microbial processes, with potential implications for carbon cycling. Our findings underscore the nonlinear and spatially variable nature of permafrost thaw effects on peatlands, emphasizing that favourable conditions for carbon sequestration may only be temporary as warming continues.

Our study's strength lies in its comprehensive and high-resolution palaeoecological methodology, which enables the detection of even subtle alterations in permafrost conditions. However, these subtle changes can rapidly escalate into dramatic landscape transformations under continued warming. Our study serves as an early warning signal of climate-induced impacts on this fragile ecosystem. Ultimately, our results demonstrate the importance of incorporating microhabitat-specific responses to warming in climate models to more accurately predict future carbon gains or losses from northern peatlands.

Data availability

The dataset underlying this study is openly available at Zenodo: 10.5281/zenodo.15543975 (Halaś et al., 2025).

Authors contribution

AH wrote the original draft, performed testate amoebae, macrocharcoal, LOI analysis, conducted all statistical analysis and prepared all figures and tables. MS performed plant macrofossil analysis, selected material for AMS radiocarbon dating and supervised the research. MO performed pollen and microcharcoal analysis. ML, DŁ, and MS collected data in the field. All authors read, reviewed, edited, and approved the final version of the manuscript.

Competing interest

The authors declare that they have no known competing financial interests or personal relationships that could have appeared to influence the work reported in this paper.

Acknowledgment

The authors thank Sergey Loiko, Alexandr O. Konstantinov, and Ivan Kritskov for help during the fieldwork, Irena Hajdas (ETH Zürich, Switzerland) for help with the age-depth model calculation, Michał Brzozowski (Poznań University of Life Sciences, Poland) for help with liverworts identification, Jerzy Jonczak (SGGW, Poland) for help with LOI analysis, Chloé Giraud (UQAM, Canada) for help with testate amoebae photos, and Harry Roberts (IGSO PAS, Poland) for English corrections. We would like to thank the reviewers for their valuable comments and constructive suggestions, which improved the quality of this manuscript.

Financial support

This study was supported by the National Science Centre in Poland (grant numbers 2019/35/O/ST10/02903 and 2021/41/B/ST10/00060), and field research at the Khanymei Research Station was possible thanks to the INTERACT (project 730938).

References

- Abbott, B. W., Jones, J. B., Schuur, E. A. G., III, F. S. C., Bowden, W. B., Bret-Harte, M. S., Epstein, H. E., Flannigan, M. D., Harms, T. K., Hollingsworth, T. N., Mack, M. C., McGuire, A. D., Natali, S. M., Rocha, A. V., Tank, S. E., Turetsky, M. R., Vonk, J. E., Wickland, K. P., Aiken, G. R., Alexander, H. D., Amon, R. M. W., Benscoter, B. W., Bergeron, Y., Bishop, K., Blarquez, O., Bond-Lamberty, B., Breen, A. L., Buffam, I., Cai, Y., Carcaillet, C., Carey, S. K., Chen, J. M., Chen, H. Y. H., Christensen, T. R., Cooper, L. W., Cornelissen, J. H. C., Groot, W. J. de, DeLuca, T. H., Dorrepaal, E., Fetcher, N., Finlay, J. C., Forbes, B. C., French, N. H. F., Gauthier, S., Girardin, M. P., Goetz, S. J., Goldammer, J. G., Gough, L., Grogan, P., Guo, L., Higuera, P. E., Hinzman, L., Hu, F. S., Hugelius, G., Jafarov, E. E., Jandt, R., Johnstone, J. F., Karlsson, J., Kasischke, E. S., Kattner, G., Kelly, R., Keuper, F., Kling, G. W., Kortelainen, P., Kouki, J., Kuhry, P., Laudon, H., Laurion, I., Macdonald, R. W., Mann, P. J., Martikainen, P. J., McClelland, J. W., Molau, U., Oberbauer, S. F., Olefeldt, D., Paré, D., Parisien, M.-A., Payette, S., Peng, C., Pokrovsky, O. S., Rastetter, E. B., Raymond, P. A., Reynolds, M. K., Rein, G., Reynolds, J. F., Robards, M., Rogers, B. M., Schädel, C., Schaefer, K., Schmidt, I. K., Shvidenko, A., Sky, J., Spencer, R. G. M., Starr, G., Striegl, R. G., Teisserenc, R., Tranvik, L. J., Virtanen, T., Welker, J. M., et al.: Biomass offsets little or none of permafrost carbon release from soils, streams, and wildfire: an expert assessment, *Environ. Res. Lett.*, 11, 034014, <https://doi.org/10.1088/1748-9326/11/3/034014>, 2016.
- Abe-Ouchi, A., Saito, F., Kageyama, M., Braconnot, P., Harrison, S. P., Lambeck, K., Otto-Bliesner, B. L., Peltier, W. R., Tarasov, L., Peterschmitt, J. Y., and Takahashi, K.: Ice-sheet configuration in the CMIP5/PMIP3 Last Glacial Maximum experiments, *Geosci Model Dev*, 8, 3621–3637, <https://doi.org/10.5194/gmd-8-3621-2015>, 2015.
- Alexandrov, G. A., Brovkin, V. A., and Kleinen, T.: The influence of climate on peatland extent in Western Siberia since the Last Glacial Maximum, *Sci. Rep.*, 6, 24784, <https://doi.org/10.1038/srep24784>, 2016.
- Baird, A. J. and Low, R. G.: The water table: Its conceptual basis, its measurement and its usefulness as a hydrological variable, *Hydrol. Process.*, 36, e14622, <https://doi.org/10.1002/hyp.14622>, 2022.
- Beilman, D. W., MacDonald, G. M., Smith, L. C., and Reimer, P. J.: Carbon accumulation in peatlands of West Siberia over the last 2000 years, *Glob. Biogeochem. Cycles*, 23, <https://doi.org/10.1029/2007GB003112>, 2009.
- Bengtsson, F., Granath, G., and Rydin, H.: Photosynthesis, growth, and decay traits in Sphagnum – a multispecies comparison, *Ecol. Evol.*, 6, 3325–3341, <https://doi.org/10.1002/ece3.2119>, 2016.
- Bengtsson, L., Semenov, V. A., and Johannessen, O. M.: The Early Twentieth-Century Warming in the Arctic—A Possible Mechanism, *J. Clim.*, 17, 4045–4057, [https://doi.org/10.1175/1520-0442\(2004\)017<4045:TETWIT>2.0.CO;2](https://doi.org/10.1175/1520-0442(2004)017<4045:TETWIT>2.0.CO;2), 2004.

- Berglund, B. E. and Ralska-Jasiewiczowa, M.: Pollen analysis and pollen diagrams, *Handb. Holocene Palaeoecol. Palaeohydrology*, 455, 484–486, 1986.
- Berner, L. T., Massey, R., Jantz, P., Forbes, B. C., Macias-fauria, M., Myers-smith, I., Kumpula, T., Gauthier, G., Andreu-hayles, L., Gaglioti, B. V., Burns, P., Zetterberg, P., D'arrigo, R., and Goetz, S. J.: Summer warming explains widespread but not uniform greening in the Arctic tundra biome, *Nat. Commun.*, 11, <https://doi.org/10.1038/s41467-020-18479-5>, 2020.
- Beug, H.-J.: *Leitfaden der Pollenbestimmung: für Mitteleuropa und angrenzende Gebiete*, Pfeil, Dr. Friedrich, Munchen, 542 pp., 2004.
- Biskaborn, B. K., Smith, S. L., Noetzli, J., Matthes, H., Vieira, G., Streletskiy, D. A., Schoeneich, P., Romanovsky, V. E., Lewkowicz, A. G., Abramov, A., Allard, M., Boike, J., Cable, W. L., Christiansen, H. H., Delaloye, R., Diekmann, B., Drozdov, D., Etzelmüller, B., Grosse, G., Guglielmin, M., Ingeman-Nielsen, T., Isaksen, K., Ishikawa, M., Johansson, M., Johannsson, H., Joo, A., Kaverin, D., Kholodov, A., Konstantinov, P., Kröger, T., Lambiel, C., Lanckman, J.-P., Luo, D., Malkova, G., Meiklejohn, I., Moskalenko, N., Oliva, M., Phillips, M., Ramos, M., Sannel, A. B. K., Sergeev, D., Seybold, C., Skryabin, P., Vasiliev, A., Wu, Q., Yoshikawa, K., Zheleznyak, M., and Lantuit, H.: Permafrost is warming at a global scale, *Nat. Commun.*, 10, 264, <https://doi.org/10.1038/s41467-018-08240-4>, 2019.
- Blockeel, T. L., Bosanquet, S. D. S., Hill, M. O., Preston, C. D., and Society, B. B.: *Atlas of British & Irish Bryophytes: The Distribution and Habitat of Mosses and Liverworts in Britain and Ireland*, Pisces Publications, 652 pp., 2014.
- Bobrov, A. A., Charman, D. J., and Warner, B. G.: Ecology of Testate Amoebae (Protozoa: Rhizopoda) on Peatlands in Western Russia with Special Attention to Niche Separation in Closely Related Taxa, *Protist*, 150, 125–136, [https://doi.org/10.1016/S1434-4610\(99\)70016-7](https://doi.org/10.1016/S1434-4610(99)70016-7), 1999.
- Bokuchava, D. D. and Semenov, V. A.: Mechanisms of the Early 20th Century Warming in the Arctic, *Earth-Sci. Rev.*, 222, 103820, <https://doi.org/10.1016/j.earscirev.2021.103820>, 2021.
- Booth, R. K., Lamentowicz, M., and Charman, D. J.: Preparation and analysis of testate amoebae in peatland palaeoenvironmental studies, *Mires Peat*, 7, 1–7, 2010.
- Borge, A. F., Westermann, S., Solheim, I., and Etzelmüller, B.: Strong degradation of palsas and peat plateaus in northern Norway during the last 60 years, *The Cryosphere*, 11, 1–16, <https://doi.org/10.5194/tc-11-1-2017>, 2017.
- Bottjer, D. J.: *Paleoecology: Past, Present and Future*, John Wiley & Sons, 272 pp., 2016.
- Brown, J., Ferrians Jr, O. J., Heginbottom, J. A., and Melnikov, E. S.: Circum-Arctic map of permafrost and ground-ice conditions, *Circum-Pac. Map*, <https://doi.org/10.3133/cp45>, 1997.
- Bulygina, O. N., Groisman, P. Y., Razuvaev, V. N., and Korshunova, N. N.: Changes in snow cover characteristics over Northern Eurasia since 1966, *Environ. Res. Lett.*, 6, 045204, <https://doi.org/10.1088/1748-9326/6/4/045204>, 2011.
- Buttler, A., Bragazza, L., Laggoun-Défarge, F., Gogo, S., Toussaint, M.-L., Lamentowicz, M., Chojnicki,

- 755 B. H., Słowiński, M., Słowińska, S., Zielińska, M., Reczuga, M., Barabach, J., Marcisz, K., Lamentowicz, Ł., Harenda, K., Lapshina, E., Gilbert, D., Schlaepfer, R., and Jassey, V. E. J.: Ericoid shrub encroachment shifts aboveground–belowground linkages in three peatlands across Europe and Western Siberia, *Glob. Change Biol.*, 29, 6772–6793, <https://doi.org/10.1111/gcb.16904>, 2023.
- Carballeira, R. and Pontevedra-Pombal, X.: Diversity of Testate Amoebae as an Indicator of the
760 Conservation Status of Peatlands in Southwest Europe, *Diversity*, 13, <https://doi.org/10.3390/d13060269>, 2021.
- Chambers, F. M. and Charman, D. J.: Holocene environmental change: contributions from the peatland archive, *The Holocene*, 14, 1–6, <https://doi.org/10.1191/0959683604hl684ed>, 2004.
- Chambers, F. M., Beilman, D. W., and Yu, Z.: Methods for determining peat humification and for
765 quantifying peat bulk density, organic matter and carbon content for palaeostudies of climate and peatland carbon dynamics., *Mires Peat*, 7, 2011.
- Charman, D. J., Hendon, D., and Woodland, W. A.: The identification of testate amoebae (Protozoa: Rhizopoda) in peats: QRA Technical Guide No. 9, Quaternary Research Asociation, London, <https://doi.org/10.1016/j.quascirev.2004.03.008>, 2000.
- 770 Charman, D. J., Blundell, A., and ACCROTELM: A new European testate amoebae transfer function for palaeohydrological reconstruction on ombrotrophic peatlands, *J. Quat. Sci.*, 22, 209–221, <https://doi.org/10.1002/jqs.1026>, 2007.
- Clymo, R. S.: The Growth of Sphagnum: Some Effects of Environment, *J. Ecol.*, 61, 849–869, <https://doi.org/10.2307/2258654>, 1973.
- 775 Conedera, M., Tinner, W., Neff, C., Meurer, M., Dickens, A. F., and Krebs, P.: Reconstructing past fire regimes: methods, applications, and relevance to fire management and conservation, *Quat. Sci. Rev.*, 28, 555–576, <https://doi.org/10.1016/j.quascirev.2008.11.005>, 2009.
- Davydova, M. I. and Rakovskaya, E. M.: Physical Geography of the USSR, *Prosveshenie*, Moscow, 1990.
- De Klerk, P., Donner, N., Joosten, H., Karpov, N. S., Minke, M., Seifert, N., and Theuerkauf, M.:
780 Vegetation patterns, recent pollen deposition and distribution of non-pollen palynomorphs in a polygon mire near Chokurdakh (NE Yakutia, NE Siberia), *Boreas*, 38, 39–58, <https://doi.org/10.1111/j.1502-3885.2008.00036.x>, 2009.
- Duchkov, A. D.: Characteristics of permafrost in Siberia, in: *Advances in the Geological Storage of Carbon Dioxide*, Dordrecht, 81–91, https://doi.org/10.1007/1-4020-4471-2_08, 2006.
- 785 Ekici, A., Lee, H., Lawrence, D. M., Swenson, S. C., and Prigent, C.: Ground subsidence effects on simulating dynamic high-latitude surface inundation under permafrost thaw using CLM5, *Geosci. Model Dev.*, 12, 5291–5300, <https://doi.org/10.5194/gmd-12-5291-2019>, 2019.
- Epstein, H. E., Myers-Smith, I., and Walker, D. A.: Recent dynamics of arctic and sub-arctic vegetation, *Environ. Res. Lett.*, 8, 015040, <https://doi.org/10.1088/1748-9326/8/1/015040>, 2013.
- 790 Faegri, K., Iversen, J., Kaland, P. E., and Krzywinski, K.: Textbook of pollen analysis, 4th ed., Blackburn

- Press, Caldwell, N.J., 328 pp., 1989.
- Fenton, N. J. and Bergeron, Y.: Sphagnum Spore Availability in Boreal Forests, *The Bryologist*, 109, 173–181, 2006.
- Feurdean, A., Gałka, M., Florescu, G., Diaconu, A.-C., Tanțău, I., Kirpotin, S., and Hutchinson, S. M.: 2000 years of variability in hydroclimate and carbon accumulation in western Siberia and the relationship with large-scale atmospheric circulation: A multi-proxy peat record, *Quat. Sci. Rev.*, 226, 105948, <https://doi.org/10.1016/j.quascirev.2019.105948>, 2019.
- Feurdean, A., Florescu, G., Tanțău, I., Vannière, B., Diaconu, A.-C., Pfeiffer, M., Warren, D., Hutchinson, S. M., Gorina, N., Gałka, M., and Kirpotin, S.: Recent fire regime in the southern boreal forests of western Siberia is unprecedented in the last five millennia, *Quat. Sci. Rev.*, 244, 106495, <https://doi.org/10.1016/j.quascirev.2020.106495>, 2020.
- Feurdean, A., Diaconu, A. C., Pfeiffer, M., Gałka, M., Hutchinson, S. M., Butiseaca, G., Gorina, N., Tonkov, S., Niamir, A., Tantau, I., Zhang, H., and Kirpotin, S.: Holocene wildfire regimes in western Siberia: interaction between peatland moisture conditions and the composition of plant functional types, *Clim Past*, 18, 1255–1274, <https://doi.org/10.5194/cp-18-1255-2022>, 2022.
- Fewster, R. E., Morris, P. J., Ivanovic, R. F., Swindles, G. T., Peregon, A. M., and Smith, C. J.: Imminent loss of climate space for permafrost peatlands in Europe and Western Siberia, *Nat. Clim. Change*, 12, 373–379, <https://doi.org/10.1038/s41558-022-01296-7>, 2022.
- Forbes, B. C., Fauria, M. M., and Zetterberg, P.: Russian Arctic warming and ‘greening’ are closely tracked by tundra shrub willows, *Glob. Change Biol.*, 16, 1542–1554, <https://doi.org/10.1111/j.1365-2486.2009.02047.x>, 2010.
- Fournier, B., Lara, E., Jassey, V. E., and Mitchell, E. A.: Functional traits as a new approach for interpreting testate amoeba palaeo-records in peatlands and assessing the causes and consequences of past changes in species composition, *The Holocene*, 25, 1375–1383, <https://doi.org/10.1177/0959683615585842>, 2015.
- Frey, K. E., Siegel, D. I., and Smith, L. C.: Geochemistry of west Siberian streams and their potential response to permafrost degradation, *Water Resour. Res.*, 43, <https://doi.org/10.1029/2006WR004902>, 2007.
- Goryushkin, L. M.: Migration, settlement and the rural economy of Siberia, 1861-1914, in: *The History of Siberia: From Russian Conquest to Revolution*, Routledge, 140–157, 1991.
- Grimm, E. C.: *Tilia and Tilia graphs computer programs*, 1991.
- Groisman, P. Y., Blyakharchuk, T. A., Chernokulsky, A. V., Arzhanov, M. M., Marchesini, L. B., Bogdanova, E. G., Borzenkova, I. I., Bulygina, O. N., Karpenko, A. A., Karpenko, L. V., Knight, R. W., Khon, V. C., Korovin, G. N., Meshcherskaya, A. V., Mokhov, I. I., Parfenova, E. I., Razuvaev, V. N., Speranskaya, N. A., Tchebakova, N. M., and Vygodskaya, N. N.: Climate Changes in Siberia, in: *Regional Environmental Changes in Siberia and Their Global Consequences*, edited by: Groisman, P. Y.

- and Gutman, G., Springer Netherlands, Dordrecht, 57–109, https://doi.org/10.1007/978-94-007-4569-8_3, 2013.
- Gurskaya, M., Hallinger, M., Singh, J., Agafonov, L., and Wilmking, M.: Temperature reconstruction in the Ob River valley based on ring widths of three coniferous tree species, *Dendrochronologia*, 30, 302–309, <https://doi.org/10.1016/j.dendro.2012.04.002>, 2012.
- Halaś, A., Lamentowicz, M., Łuców, D., and Słowiński, M.: Developing a new testate amoeba hydrological transfer function for permafrost peatlands of NW Siberia, *Quat. Sci. Rev.*, 308, 108067, <https://doi.org/10.1016/j.quascirev.2023.108067>, 2023.
- Halaś, A., Lamentowicz, M., Obremska, M., Łuców, D., and Słowiński, M.: Data from: Peatland development reconstruction and complex biological responses to permafrost thawing in Western Siberia, <https://doi.org/10.5281/zenodo.15543975>, 2025.
- Hantemirov, R. M., Corona, C., Guillet, S., Shiyatov, S. G., Stoffel, M., Osborn, T. J., Melvin, T. M., Gorlanova, L. A., Kukarskih, V. V., Surkov, A. Y., von Arx, G., and Fonti, P.: Current Siberian heating is unprecedented during the past seven millennia, *Nat. Commun.*, 13, 4968, <https://doi.org/10.1038/s41467-022-32629-x>, 2022.
- Harris, L. I., Moore, T. R., Roulet, N. T., and Pinsonneault, A. J.: Lichens: A limit to peat growth?, *J. Ecol.*, 106, 2301–2319, <https://doi.org/10.1111/1365-2745.12975>, 2018.
- Harris, L. I., Olefeldt, D., Pelletier, N., Blodau, C., Knorr, K.-H., Talbot, J., Heffernan, L., and Turetsky, M.: Permafrost thaw causes large carbon loss in boreal peatlands while changes to peat quality are limited, *Glob. Change Biol.*, n/a, <https://doi.org/10.1111/gcb.16894>, 2023.
- Heffernan, L., Estop-Aragonés, C., Knorr, K.-H., Talbot, J., and Olefeldt, D.: Long-term Impacts of Permafrost Thaw on Carbon Storage in Peatlands: Deep Losses Offset by Surficial Accumulation, *J. Geophys. Res. Biogeosciences*, 125, e2019JG005501, <https://doi.org/10.1029/2019JG005501>, 2020.
- Heiri, O., Lotter, A. F., and Lemcke, G.: Loss on ignition as a method for estimating organic and carbonate content in sediments: reproducibility and comparability of results, *J. Paleolimnol.*, 25, 101–110, <https://doi.org/10.1023/A:1008119611481>, 2001.
- Hua, Q., Barbetti, M., and Rakowski, A. Z.: Atmospheric Radiocarbon for the Period 1950–2010, *Radiocarbon*, 55, 2059–2072, https://doi.org/10.2458/azu_js_rc.v55i2.16177, 2013.
- Hugelius, G., Loisel, J., Chadburn, S., Jackson, R. B., Jones, M., MacDonald, G., Marushchak, M., Olefeldt, D., Packalen, M., Siewert, M. B., Treat, C., Turetsky, M., Voigt, C., and Yu, Z.: Large stocks of peatland carbon and nitrogen are vulnerable to permafrost thaw, *Proc. Natl. Acad. Sci.*, 117, 20438–20446, <https://doi.org/10.1073/pnas.1916387117>, 2020.
- Hunter, J. D.: Matplotlib: A 2D Graphics Environment, *Comput. Sci. Eng.*, 9, 90–95, <https://doi.org/10.1109/MCSE.2007.55>, 2007.
- Inglis, G., Collinson, M., Wilde, V., Riegel, W., Robson, B., Lenz, O., and Pancost, R.: Ecological and biogeochemical change in an early Paleogene peat-forming environment: Linking biomarkers and

- palynology, *Palaeogeogr. Palaeoclimatol. Palaeoecol.*, 438, <https://doi.org/10.1016/j.palaeo.2015.08.001>, 2015.
- 865 IPCC: Climate Change 2021 – The Physical Science Basis: Working Group I Contribution to the Sixth Assessment Report of the Intergovernmental Panel on Climate Change, Cambridge University Press, Cambridge, <https://doi.org/10.1017/9781009157896>, 2023.
- Jacquemart, A.-L.: *Andromeda polifolia* L., *J. Ecol.*, 86, 527–541, <https://doi.org/10.1046/j.1365-2745.1998.00274.x>, 1998.
- 870 Jeong, S.-J., Bloom, A. A., Schimel, D., Sweeney, C., Parazoo, N. C., Medvigy, D., Schaepman-Strub, G., Zheng, C., Schwalm, C. R., Huntzinger, D. N., Michalak, A. M., and Miller, C. E.: Accelerating rates of Arctic carbon cycling revealed by long-term atmospheric CO₂ measurements, *Sci. Adv.*, 4, eaao1167, <https://doi.org/10.1126/sciadv.aao1167>, 2018.
- Juggins, S.: C2 Version 1.5. Software for ecological and palaeoecological data analysis and visualisation, 875 2007.
- Juggins, S.: rioja: Analysis of Quaternary Science Data, R package version 0.9-26, 2020.
- Karlsson, J., Serikova, S., Vorobyev, S. N., Rocher-Ros, G., Denfeld, B., and Pokrovsky, O. S.: Carbon emission from Western Siberian inland waters, *Nat. Commun.*, 12, 825, <https://doi.org/10.1038/s41467-021-21054-1>, 2021.
- 880 Katz, N. J., Katz, S. V., and Skobiejeva, E. I.: Atlas rastitielnykh ostatkov v torfach, Nedra, Moscow, Russia, 370 pp., 1977.
- Kluge, M., Wauthy, M., Clemmensen, K. E., Wurzbacher, C., Hawkes, J. A., Einarsdottir, K., Rautio, M., Stenlid, J., and Peura, S.: Declining fungal diversity in Arctic freshwaters along a permafrost thaw gradient, *Glob. Change Biol.*, 27, 5889–5906, <https://doi.org/10.1111/gcb.15852>, 2021.
- 885 Kondratjeva, K. A., Khrutsky, S. F., and Romanovsky, N. N.: Changes in the extent of permafrost during the late quaternary period in the territory of the former Soviet Union, *Permafr. Periglac. Process.*, 4, 113–119, <https://doi.org/10.1002/ppp.3430040204>, 1993.
- Kremenetski, K. V., Velichko, A. A., Borisova, O. K., MacDonald, G. M., Smith, L. C., Frey, K. E., and Orlova, L. A.: Peatlands of the Western Siberian lowlands: current knowledge on zonation, carbon content and Late Quaternary history, *Quat. Sci. Rev.*, 22, 703–723, [https://doi.org/10.1016/S0277-3791\(02\)00196-8](https://doi.org/10.1016/S0277-3791(02)00196-8), 2003.
- 890 Kuhry, P.: The palaeoecology of a treed bog in western boreal Canada: a study based on microfossils, macrofossils and physico-chemical properties, *Rev. Palaeobot. Palynol.*, 96, 183–224, [https://doi.org/10.1016/S0034-6667\(96\)00018-8](https://doi.org/10.1016/S0034-6667(96)00018-8), 1997.
- 895 Kujala, K., Seppälä, M., and Holappa, T.: Physical properties of peat and palsa formation, *Cold Reg. Sci. Technol.*, 52, 408–414, <https://doi.org/10.1016/j.coldregions.2007.08.002>, 2008.
- Kulczyński, S.: *Torfowiska Polesia*, PUA 37, Kraków, 1939.
- Kuosmanen, N., Välimäki, M., Piilo, S., Tuittila, E.-S., Oksanen, P., and Wallenius, T.: Repeated fires in

- forested peatlands in sporadic permafrost zone in Western Canada, *Environ. Res. Lett.*, 18, 094051, <https://doi.org/10.1088/1748-9326/acf05b>, 2023.
- Kurina, I. V., Veretennikova, E. E., Il'ina, A. A., Egorova, M. L., Salisch, L. V., Dolgin, V. N., Udaloj, A. V., Golovatskaya, E. A., Dyukarev, E. A., and Smirnov, S. V.: Multi-proxy climate and environmental records from a Holocene eutrophic mire, southern taiga subzone, West Siberia, *Boreas*, 52, 223–239, <https://doi.org/10.1111/bor.12604>, 2023.
- Kurz, W. A., Dymond, C. C., Stinson, G., Rampley, G. J., Neilson, E. T., Carroll, A. L., Ebata, T., and Safranyik, L.: Mountain pine beetle and forest carbon feedback to climate change, *Nature*, 452, 987–990, <https://doi.org/10.1038/nature06777>, 2008.
- Laliberté, E., Legendre, P., and Shipley, B.: FD: measuring functional diversity from multiple traits, and other tools for functional ecology. R package version 1.0-12.1., 2014.
- Lamarre, A., Garneau, M., and Asnong, H.: Holocene paleohydrological reconstruction and carbon accumulation of a permafrost peatland using testate amoeba and macrofossil analyses, Kuujuarapik, subarctic Québec, Canada, *Rev. Palaeobot. Palynol.*, 186, 131–141, <https://doi.org/10.1016/j.revpalbo.2012.04.009>, 2012.
- Lamentowicz, M., Milecka, K., Gałka, M., Cedro, A., Pawlyta, J., Piotrowska, N., Lamentowicz, Ł., and Van Der Knaap, W. O.: Climate and human induced hydrological change since AD 800 in an ombrotrophic mire in Pomerania (N Poland) tracked by testate amoebae, macro-fossils, pollen and tree rings of pine, *Boreas*, 38, 214–229, <https://doi.org/10.1111/j.1502-3885.2008.00047.x>, 2009.
- Lamentowicz, M., Słowiński, M., Marcisz, K., Ziełńska, M., Kaliszan, K., Lapshina, E., Gilbert, D., Buttler, A., Fiałkiewicz-Kozieł, B., Jassey, V. E. J., Laggoun-Defarge, F., and Kołaczek, P.: Hydrological dynamics and fire history of the last 1300 years in western Siberia reconstructed from a high-resolution, ombrotrophic peat archive, *Quat. Res.*, 84, 312–325, <https://doi.org/10.1016/j.yqres.2015.09.002>, 2015.
- Lamentowicz, M., Kajukało-Drygalska, K., Kołaczek, P., Jassey, V. E. J., Gąbka, M., and Karpińska-Kołaczek, M.: Testate amoebae taxonomy and trait diversity are coupled along an openness and wetness gradient in pine-dominated Baltic bogs, *Eur. J. Protistol.*, 73, 125674, <https://doi.org/10.1016/j.ejop.2020.125674>, 2020.
- Lawrence, D. M., Koven, C. D., Swenson, S. C., Riley, W. J., and Slater, A. G.: Permafrost thaw and resulting soil moisture changes regulate projected high-latitude CO₂ and CH₄ emissions, *Environ. Res. Lett.*, 10, 094011, <https://doi.org/10.1088/1748-9326/10/9/094011>, 2015.
- Li, J., Holmgren, M., and Xu, C.: Greening vs browning? Surface water cover mediates how tundra and boreal ecosystems respond to climate warming, *Environ. Res. Lett.*, 16, 104004, <https://doi.org/10.1088/1748-9326/ac2376>, 2021.
- Luoto, M. and Seppälä, M.: Thermokarst ponds as indicators of the former distribution of palsas in Finnish Lapland, *Permafr. Periglac. Process.*, 14, 19–27, <https://doi.org/10.1002/ppp.441>, 2003.
- Magnússon, R. Í., Groten, F., Bartholomeus, H., van Huissteden, K., and Heijmans, M. M. P. D.: Tundra

- 935 Browning in the Indigirka Lowlands (North-Eastern Siberia) Explained by Drought, Floods and Small-Scale Vegetation Shifts, *J. Geophys. Res. Biogeosciences*, 128, e2022JG007330, <https://doi.org/10.1029/2022JG007330>, 2023.
- Malmer, N.: Patterns in the Growth and the Accumulation of Inorganic Constituents in the Sphagnum Cover on Ombrotrophic Bogs in Scandinavia, *Oikos*, 53, 105, <https://doi.org/10.2307/3565670>, 1988.
- 940 Malmer, N.: On the relations between water regime, mass accretion and formation of ombrotrophic conditions in Sphagnum mires, *Mires Peat*, 14, 1–23, 2014.
- Manasypov, R. M., Shirokova, L. S., and Pokrovsky, O. S.: Experimental modeling of thaw lake water evolution in discontinuous permafrost zone: Role of peat, lichen leaching and ground fire, *Sci. Total Environ.*, 580, 245–257, <https://doi.org/10.1016/j.scitotenv.2016.12.067>, 2017.
- 945 Mann, M.: Little Ice Age, *Encycl. Glob. Environ. Change*, 2002.
- Marcisz, K., Tinner, W., Colombaroli, D., Kołaczek, P., Słowiński, M., Fiałkiewicz-Kozieł, B., Łokas, E., and Lamentowicz, M.: Long-term hydrological dynamics and fire history over the last 2000 years in CE Europe reconstructed from a high-resolution peat archive, *Quat. Sci. Rev.*, 112, 138–152, <https://doi.org/10.1016/j.quascirev.2015.01.019>, 2015.
- 950 Markkula, I., Oksanen, P., and Kuhry, P.: Indicator value of oribatid mites in determining past permafrost dynamics in northern European sub-Arctic peatlands, *Boreas*, 47, 884–896, <https://doi.org/10.1111/bor.12312>, 2018.
- Martini, I. P., Cortizas, A. M., and Chesworth, W.: *Peatlands: Evolution and Records of Environmental and Climate Changes*, Elsevier, 606 pp., 2007.
- 955 Mauquoy, D. and Geel, B.: Mire and peat macros, in: *Encyclopedia of Quaternary Science*, vol. 3, Elsevier, Amsterdam, 2315–2336, 2007.
- Mekonnen, Z. A., Riley, W. J., Berner, L. T., Bouskill, N. J., Torn, M. S., Iwahana, G., Breen, A. L., Myers-Smith, I. H., Criado, M. G., Liu, Y., Euskirchen, E. S., Goetz, S. J., Mack, M. C., and Grant, R. F.: Arctic tundra shrubification: a review of mechanisms and impacts on ecosystem carbon balance, *Environ. Res. Lett.*, 16, 053001, <https://doi.org/10.1088/1748-9326/abf28b>, 2021.
- 960 Miles, V. V. and Esau, I.: Spatial heterogeneity of greening and browning between and within bioclimatic zones in northern West Siberia, *Environ. Res. Lett.*, 11, 115002, <https://doi.org/10.1088/1748-9326/11/11/115002>, 2016.
- Mitchell, E. A. D., Buttler, A., Grosvernier, P., Rydin, H., Albinsson, C., Greenup, A. L., Heijmans, M.
- 965 M. P. D., Hoosbeek, M. R., and Saarinen, T.: Relationships among testate amoebae (Protozoa), vegetation and water chemistry in five Sphagnum-dominated peatlands in Europe, *New Phytol.*, 145, 95–106, <https://doi.org/10.1046/j.1469-8137.2000.00550.x>, 2000.
- Mitchell, E. A. D., Gilbert, D., Buttler, A., Amblard, C., Grosvernier, P., and Gobat, J. M.: Structure of Microbial Communities in Sphagnum Peatlands and Effect of Atmospheric Carbon Dioxide Enrichment, *Microb. Ecol.*, 46, 187–199, 2003.
- 970

Mitchell, E. A. D., Payne, R. J., and Lamentowicz, M.: Potential implications of differential preservation of testate amoeba shells for paleoenvironmental reconstruction in peatlands, *J. Paleolimnol.*, 40, 603–618, <https://doi.org/10.1007/s10933-007-9185-z>, 2008.

975 Mooney, S. and Radford, K.: A simple and fast method for the quantification of macroscopic charcoal from sediments, *Quat. Australas.*, 19, 43–46, 2001.

Moore, P. D., Collinson, M., and Webb, J. A.: *Pollen Analysis*, 2nd edition., Wiley, 216 pp., 1994.

Myers-Smith, I. H., Kerby, J. T., Phoenix, G. K., Bjerke, J. W., Epstein, H. E., Assmann, J. J., John, C., Andreu-Hayles, L., Angers-Blondin, S., Beck, P. S. A., Berner, L. T., Bhatt, U. S., Bjorkman, A. D., Blok, D., Bryn, A., Christiansen, C. T., Cornelissen, J. H. C., Cunliffe, A. M., Elmendorf, S. C., Forbes, B. C.,
980 Goetz, S. J., Hollister, R. D., de Jong, R., Loranty, M. M., Macias-Fauria, M., Maseyk, K., Normand, S., Olofsson, J., Parker, T. C., Parmentier, F.-J. W., Post, E., Schaepman-Strub, G., Stordal, F., Sullivan, P. F., Thomas, H. J. D., Tømmervik, H., Treharne, R., Tweedie, C. E., Walker, D. A., Wilmking, M., and Wipf, S.: Complexity revealed in the greening of the Arctic, *Nat. Clim. Change*, 10, 106–117, <https://doi.org/10.1038/s41558-019-0688-1>, 2020.

985 Naumov, I. V.: *The History of Siberia*, Routledge, 242 pp., 2009.

Nelson, K., Thompson, D., Hopkinson, C., Petrone, R., and Chasmer, L.: Peatland-fire interactions: A review of wildland fire feedbacks and interactions in Canadian boreal peatlands, *Sci. Total Environ.*, 769, 145212, <https://doi.org/10.1016/j.scitotenv.2021.145212>, 2021.

Neustadt, M. I.: On absolute age of peat bogs of Western Siberia., *Rev. Roum. Biol. Ser. Bot.*, 12, 181–
990 186, 1967.

Novenko, E. Y., Mazei, N. G., Kupriyanov, D. A., Babeshko, K. V., Kusilman, M. V., Zyuganova, I. S., Tsyganov, A. N., Mazei, Y. A., Phelps, L. N., and Davis, B. A.: A 1300-year multi-proxy palaeoecological record from the northwest Putorana Plateau (Russian Subarctic): environmental changes, vegetation dynamics and fire history, *The Holocene*, 33, 181–193, <https://doi.org/10.1177/09596836221131693>,
995 2023.

Nungesser, M. K.: Modelling microtopography in boreal peatlands: hummocks and hollows, *Ecol. Model.*, 165, 175–207, [https://doi.org/10.1016/S0304-3800\(03\)00067-X](https://doi.org/10.1016/S0304-3800(03)00067-X), 2003.

Ogden, C. G. and Hedley, R. H.: *An Atlas of Freshwater Testate Amoebae*, Oxford University Press [for the] British Museum (Natural History), 236 pp., 1980.

1000 Ogden, E. L., Cumming, S. G., Smith, S. L., Turetsky, M. R., and Baltzer, J. L.: Permafrost thaw induces short-term increase in vegetation productivity in northwestern Canada, *Glob. Change Biol.*, 29, 5352–5366, <https://doi.org/10.1111/gcb.16812>, 2023.

Oksanen, J., Simpson, G., Blanchet, F., Kindt, R., Legendre, P., Minchin, P., O'Hara, R., Solymos, P., Stevens, M., Szoecs, E., Wagner, H., Barbour, M., Bedward, M., Bolker, B., Borcard, D., Carvalho, G.,
1005 Chirico, M., De Caceres, M., Durand, S., Evangelista, H., FitzJohn, R., Friendly, M., Furneaux, B., Hannigan, G., Hill, M., Lahti, L., McGlinn, D., Ouellette, M., Ribeiro Cunha, E., Smith, T., Stier, A., Ter

Braak, C., and Weedon, J.: *vegan: Community Ecology Package*. R package version 2.6-2, 2022.

Olefeldt, D., Heffernan, L., Jones, M. C., Sannel, A. B. K., Treat, C. C., and Turetsky, M. R.: Permafrost Thaw in Northern Peatlands: Rapid Changes in Ecosystem and Landscape Functions, in: *Ecosystem Collapse and Climate Change*, edited by: Canadell, J. G. and Jackson, R. B., Springer International Publishing, Cham, 27–67, https://doi.org/10.1007/978-3-030-71330-0_3, 2021.

O'Neill, H. B., Smith, S. L., Burn, C. R., Duchesne, C., and Zhang, Y.: Widespread Permafrost Degradation and Thaw Subsidence in Northwest Canada, *J. Geophys. Res. Earth Surf.*, 128, e2023JF007262, <https://doi.org/10.1029/2023JF007262>, 2023.

Pandey, A., Tripathi, S., and Basumatary, S.: Non-Pollen Palynomorphs from the Late-Holocene Sediments of Majuli Island, Assam (Indo-Burma Region): Implications to Palaeoenvironmental Studies, 63–81, https://doi.org/10.1007/978-3-031-13119-6_5, 2023.

Pedregosa, F., Varoquaux, G., Gramfort, A., Michel, V., Thirion, B., Grisel, O., Blondel, M., Prettenhofer, P., Weiss, R., Dubourg, V., Vanderplas, J., Passos, A., Cournapeau, D., Brucher, M., Perrot, M., and Duchesnay, É.: *Scikit-learn: Machine Learning in Python*, *J. Mach. Learn. Res.*, 12, 2825–2830, 2011.

Peel, M. C., Finlayson, B. L., and McMahon, T. A.: Updated world map of the Köppen-Geiger climate classification, *Hydrol Earth Syst Sci*, 11, 1633–1644, <https://doi.org/10.5194/hess-11-1633-2007>, 2007.

Pelletier, N., Talbot, J., Olefeldt, D., Turetsky, M., Blodau, C., Sonnentag, O., and Quinton, W. L.: Influence of Holocene permafrost aggradation and thaw on the paleoecology and carbon storage of a peatland complex in northwestern Canada, *The Holocene*, 27, 1391–1405, <https://doi.org/10.1177/0959683617693899>, 2017.

Peteet, D., Andreev, A., Bardeen, W., and Mistretta, F.: Long-term Arctic peatland dynamics, vegetation and climate history of the Pur-Taz region, Western Siberia, *Boreas*, 27, 115–126, <https://doi.org/10.1111/j.1502-3885.1998.tb00872.x>, 1998.

Philben, M., Kaiser, K., and Benner, R.: Biochemical evidence for minimal vegetation change in peatlands of the West Siberian Lowland during the Medieval Climate Anomaly and Little Ice Age, *J. Geophys. Res. Biogeosciences*, 119, 808–825, <https://doi.org/10.1002/2013JG002396>, 2014.

Phoenix, G. K. and Bjerke, J. W.: Arctic browning: extreme events and trends reversing arctic greening, *Glob. Change Biol.*, 22, 2960–2962, <https://doi.org/10.1111/gcb.13261>, 2016.

Polishchuk, Y. M., Bryksina, N. A., and Polishchuk, V. Y.: Remote analysis of changes in the number of small thermokarst lakes and their distribution with respect to their sizes in the cryolithozone of Western Siberia, 2015, *Izv. Atmospheric Ocean. Phys.*, 51, 999–1006, <https://doi.org/10.1134/S0001433815090145>, 2015.

Qin, Y., Li, H., Mazei, Y., Kurina, I., Swindles, G. T., Bobrov, A., Tsyganov, A. N., Gu, Y., Huang, X., Xue, J., Lamentowicz, M., Marcisz, K., Roland, T., Payne, R. J., Mitchell, E. A. D., and Xie, S.: Developing a continental-scale testate amoeba hydrological transfer function for Asian peatlands, *Quat. Sci. Rev.*, 258, 106868, <https://doi.org/10.1016/j.quascirev.2021.106868>, 2021.

R Core Team: R: A language and environment for statistical computing, 2022.

Railton, J. B. and Sparling, J. H.: Preliminary studies on the ecology of palsa mounds in northern Ontario,
1045 Can. J. Bot., 51, 1037–1044, <https://doi.org/10.1139/b73-128>, 1973.

Ramsey, C. B.: Development of the Radiocarbon Calibration Program, Radiocarbon, 43, 355–363,
<https://doi.org/10.1017/S0033822200038212>, 2001.

Rantanen, M., Karpechko, A. Y., Lipponen, A., Nordling, K., Hyvärinen, O., Ruosteenoja, K., Vihma,
T., and Laaksonen, A.: The Arctic has warmed nearly four times faster than the globe since 1979,
1050 Commun. Earth Environ., 3, 1–10, <https://doi.org/10.1038/s43247-022-00498-3>, 2022.

Raudina, T. V., Loiko, S. V., Lim, A. G., Krickov, I. V., Shirokova, L. S., Istigechev, G. I., Kuzmina, D.
M., Kulizhsky, S. P., Vorobyev, S. N., and Pokrovsky, O. S.: Dissolved organic carbon and major and
trace elements in peat porewater of sporadic, discontinuous, and continuous permafrost zones of western
Siberia, Biogeosciences, 14, 3561–3584, <https://doi.org/10.5194/bg-14-3561-2017>, 2017.

Reimer, P. J., Austin, W. E. N., Bard, E., Bayliss, A., Blackwell, P. G., Ramsey, C. B., Butzin, M., Cheng,
H., Edwards, R. L., Friedrich, M., Grootes, P. M., Guilderson, T. P., Hajdas, I., Heaton, T. J., Hogg, A.
G., Hughen, K. A., Kromer, B., Manning, S. W., Muscheler, R., Palmer, J. G., Pearson, C., Plicht, J. van
der, Reimer, R. W., Richards, D. A., Scott, E. M., Southon, J. R., Turney, C. S. M., Wacker, L., Adolphi,
F., Büntgen, U., Capano, M., Fahrni, S. M., Fogtmann-Schulz, A., Friedrich, R., Köhler, P., Kudsk, S.,
1060 Miyake, F., Olsen, J., Reinig, F., Sakamoto, M., Sookdeo, A., and Talamo, S.: The IntCal20 Northern
Hemisphere Radiocarbon Age Calibration Curve (0–55 cal kBP), Radiocarbon, 62, 725–757,
<https://doi.org/10.1017/RDC.2020.41>, 2020.

Romanovsky, V. E., Drozdov, D. S., Oberman, N. G., Malkova, G. V., Kholodov, A. L., Marchenko, S.
S., Moskalenko, N. G., Sergeev, D. O., Ukraintseva, N. G., Abramov, A. A., Gilichinsky, D. A., and
1065 Vasiliev, A. A.: Thermal state of permafrost in Russia, Permafr. Periglac. Process., 21, 136–155,
<https://doi.org/10.1002/ppp.683>, 2010.

Rönkkö, M. and Seppälä, M.: Surface characteristics affecting active layer formation in palsas, Finnish
Lapland, 2003.

Rydin, H. and Jeglum, J. K.: Peatland habitats, in: The Biology of Peatlands, edited by: Rydin, H. and
1070 Jeglum, J. K., Oxford University Press, 1–20,
<https://doi.org/10.1093/acprof:osobl/9780199602995.003.0001>, 2013.

Safronova, I. and Yurkovskysya, T.: The latitudinal distribution of vegetation cover in Siberia, BIO Web
Conf, 16, 00047, 2019.

Sannel, A. B. K. and Kuhry, P.: Long-term stability of permafrost in subarctic peat plateaus, west-central
1075 Canada, The Holocene, 18, 589–601, <https://doi.org/10.1177/0959683608089658>, 2008.

Sannel, A. B. K. and Kuhry, P.: Holocene peat growth and decay dynamics in sub-arctic peat plateaus,
west-central Canada, Boreas, 38, 13–24, <https://doi.org/10.1111/j.1502-3885.2008.00048.x>, 2009.

Sannel, A. B. K. and Kuhry, P.: Warming-induced destabilization of peat plateau/thermokarst lake

complexes, *J. Geophys. Res. Biogeosciences*, 116, <https://doi.org/10.1029/2010JG001635>, 2011.

1080 Schuur, E. A. G., McGuire, A. D., Schädel, C., Grosse, G., Harden, J. W., Hayes, D. J., Hugelius, G., Koven, C. D., Kuhry, P., Lawrence, D. M., Natali, S. M., Olefeldt, D., Romanovsky, V. E., Schaefer, K., Turetsky, M. R., Treat, C. C., and Vonk, J. E.: Climate change and the permafrost carbon feedback, *Nature*, 520, 171–179, <https://doi.org/10.1038/nature14338>, 2015.

Schuur, E. A. G., Pallandt, M., and Göckede, M.: Russian collaboration loss risks permafrost carbon emissions network, *Nat. Clim. Change*, 14, 410–411, <https://doi.org/10.1038/s41558-024-02001-6>, 2024.

1085 Seneviratne, S. I., Zhang, X., Adnan, M., Badi, W., Dereczynski, C., Di Luca, A., Ghosh, S., Iskandar, I., Kossin, J., Lewis, S., Otto, F., Pinto, I., Satoh, M., Vicente-Serrano, S. M., Wehner, M., and Zhou, B.: Weather and Climate Extreme Events in a Changing Climate, in: *Climate Change 2021: The Physical Science Basis. Contribution of Working Group I to the Sixth Assessment Report of the Intergovernmental Panel on Climate Change*, edited by: Pörtner, H.-O., Roberts, D. C., Tignor, M., Poloczanska, E. S., Mintenbeck, K., Alegria, A., Craig, M., Langsdorf, S., Löschke, S., Möller, V., Okem, A., and B., R., Cambridge University Press, Cambridge, United Kingdom and New York, NY, USA, 1513–1766, <https://doi.org/10.1017/9781009157896.013>, 2021.

1090 Seppälä, M.: Palsas and related forms, in: *Advances in Periglacial Geomorphology*, John Wiley and Sons, New York, 247–78, 1988.

1095 Seppälä, M.: Synthesis of studies of palsa formation underlining the importance of local environmental and physical characteristics, *Quat. Res.*, 75, 366–370, <https://doi.org/10.1016/j.yqres.2010.09.007>, 2011.

Sheng, Y., Smith, L. C., MacDonald, G. M., Kremenetski, K. V., Frey, K. E., Velichko, A. A., Lee, M., Beilman, D. W., and Dubinin, P.: A high-resolution GIS-based inventory of the west Siberian peat carbon pool, *Glob. Biogeochem. Cycles*, 18, <https://doi.org/10.1029/2003GB002190>, 2004.

1100 Shumilovskikh, L., Schlütz, F., Achterberg, I., Bauerochse, A., and Leuschner, H.: Non-Pollen Palynomorphs from Mid-Holocene Peat of the Raised Bog Borsteler Moor (Lower Saxony, Germany), *Stud. Quat.*, 32, 5–18, <https://doi.org/10.1515/squa-2015-0001>, 2015.

Shumilovskikh, L., O’Keefe, J. M. K., and Marret, F.: An overview of the taxonomic groups of non-pollen palynomorphs, *Geol. Soc. Lond. Spec. Publ.*, 511, 13–61, <https://doi.org/10.1144/SP511-2020-65>, 2021.

Shur, Y. L. and Jorgenson, M. T.: Patterns of permafrost formation and degradation in relation to climate and ecosystems, *Permafr. Periglac. Process.*, 18, 7–19, <https://doi.org/10.1002/ppp.582>, 2007.

Siemensma, F. J.: *Microworld, world of amoeboid organisms*. World-wide electronic publication, 2022.

1110 Sillasoo, Ü., Väliiranta, M., and Tuittila, E.-S.: Fire history and vegetation recovery in two raised bogs at the Baltic Sea, *J. Veg. Sci.*, 22, 1084–1093, <https://doi.org/10.1111/j.1654-1103.2011.01307.x>, 2011.

Sim, T. G., Swindles, G. T., Morris, P. J., Baird, A. J., Cooper, C. L., Gallego-Sala, A. V., Charman, D. J., Roland, T. P., Borken, W., Mullan, D. J., Aquino-López, M. A., and Galka, M.: Divergent responses of permafrost peatlands to recent climate change, *Environ. Res. Lett.*, 16, 034001,

- 1115 <https://doi.org/10.1088/1748-9326/abe00b>, 2021.
- Singh, S. P., Gumber, S., Singh, R. D., and Pandey, R.: Differentiation of diploxylon and haploxylon pines in spatial distribution, and adaptational traits, *Acta Ecol. Sin.*, 43, 1–10, <https://doi.org/10.1016/j.chnaes.2021.07.007>, 2023.
- Smith, L. C., MacDonald, G. M., Velichko, A. A., Beilman, D. W., Borisova, O. K., Frey, K. E.,
1120 Kremenetski, K. V., and Sheng, Y.: Siberian Peatlands a Net Carbon Sink and Global Methane Source Since the Early Holocene, *Science*, 303, 353–356, <https://doi.org/10.1126/science.1090553>, 2004.
- Smith, L. C., Sheng, Y., MacDonald, G. M., and Hinzman, L. D.: Disappearing Arctic Lakes, *Science*, 308, 1429–1429, <https://doi.org/10.1126/science.1108142>, 2005.
- Smith, S. L., O'Neill, H. B., Isaksen, K., Noetzli, J., and Romanovsky, V. E.: The changing thermal state
1125 of permafrost, *Nat. Rev. Earth Environ.*, 3, 10–23, <https://doi.org/10.1038/s43017-021-00240-1>, 2022.
- Spiller, A., Kallenbach, C. M., Burnett, M. S., Olefeldt, D., Schulze, C., Maranger, R., and Douglas, P. M. J.: Gradual drying of permafrost peat decreases carbon dioxide in drier peat plateaus but not in wetter fens and bogs, *EGUspHERE*, 1–15, <https://doi.org/10.5194/egusphere-2024-2248>, 2024.
- Standen, K. M. and Baltzer, J. L.: Permafrost condition determines plant community composition and
1130 community-level foliar functional traits in a boreal peatland, *Ecol. Evol.*, 11, 10133–10146, <https://doi.org/10.1002/ece3.7818>, 2021.
- Stockmarr, J.: Tablets with Spores used in Absolute Pollen Analysis, *Pollen Spores*, 13, 615–621, 1971.
- Street, L. E., Subke, J.-A., Sommerkorn, M., Sloan, V., Ducrottoy, H., Phoenix, G. K., and Williams, M.: The role of mosses in carbon uptake and partitioning in arctic vegetation, *New Phytol.*, 199, 163–175,
1135 <https://doi.org/10.1111/nph.12285>, 2013.
- Streletskiy, D., Anisimov, O., and Vasiliev, A.: Permafrost Degradation, in: *Snow and Ice-Related Hazards, Risks, and Disasters*, edited by: Shroder, J. F., Haeberli, W., and Whiteman, C., Academic Press, Boston, 303–344, <https://doi.org/10.1016/B978-0-12-394849-6.00010-X>, 2015.
- Swindles, G. T., Morris, P. J., Mullan, D., Watson, E. J., Turner, T. E., Roland, T. P., Amesbury, M. J.,
1140 Kokfelt, U., Schoning, K., Pratte, S., Gallego-Sala, A., Charman, D. J., Sanderson, N., Garneau, M., Carrivick, J. L., Woulds, C., Holden, J., Parry, L., and Galloway, J. M.: The long-term fate of permafrost peatlands under rapid climate warming, *Sci. Rep.*, 5, 17951, <https://doi.org/10.1038/srep17951>, 2015.
- Thibault, S. and Payette, S.: Recent permafrost degradation in bogs of the James Bay area, northern Quebec, Canada, *Permafr. Periglac. Process.*, 20, 383–389, <https://doi.org/10.1002/ppp.660>, 2009.
- 1145 Thompson, D. K. and Waddington, J. M.: Sphagnum under pressure: towards an ecohydrological approach to examining Sphagnum productivity, *Ecohydrology*, 1, 299–308, <https://doi.org/10.1002/eco.31>, 2008.
- Tikhonravova, Y., Kuznetsova, A., Slagoda, E., and Koroleva, E.: Holocene permafrost peatland evolution in drained lake basins on the Pur-Taz Interfluvium, North-Western Siberia, *Quat. Int.*,
1150 <https://doi.org/10.1016/j.quaint.2023.07.005>, 2023.

Tobolski, K.: Przewodnik do oznaczania torfów i osadów jeziornych, Wydawnictwo Naukowe PWN, Warszawa, 2000.

Todorov, M. and Bankov, N.: An Atlas of Sphagnum-Dwelling Testate Amoebae in Bulgaria, 1st ed., Pensoft Publishers, Sofia, Bulgaria, Advanced Books pp., <https://doi.org/10.3897/ab.e38685>, 2019.

1155 Tolonen, K. and Turunen, J.: Accumulation rates of carbon in mires in Finland and implications for climate change, *The Holocene*, 6, 171–178, <https://doi.org/10.1177/095968369600600204>, 1996.

Treat, C. C. and Jones, M. C.: Near-surface permafrost aggradation in Northern Hemisphere peatlands shows regional and global trends during the past 6000 years, *The Holocene*, 28, 998–1010, <https://doi.org/10.1177/0959683617752858>, 2018.

1160 Treat, C. C., Jones, M. C., Camill, P., Gallego-Sala, A., Garneau, M., Harden, J. W., Hugelius, G., Klein, E. S., Kokfelt, U., Kuhry, P., Loisel, J., Mathijssen, P. J. H., O'Donnell, J. A., Oksanen, P. O., Ronkainen, T. M., Sannel, A. B. K., Talbot, J., Tarnocai, C., and Väiranta, M.: Effects of permafrost aggradation on peat properties as determined from a pan-Arctic synthesis of plant macrofossils, *J. Geophys. Res. Biogeosciences*, 121, 78–94, <https://doi.org/10.1002/2015JG003061>, 2016.

1165 Trofimova, I. E. and Balybina, A. S.: Classification of climates and climatic regionalization of the West-Siberian plain, *Geogr. Nat. Resour.*, 35, 114–122, <https://doi.org/10.1134/S1875372814020024>, 2014.

Vaguet, Y.: Oil and Gas towns in Western Siberia: past, present and future challenges, *Nordregio*, WP 6:218, 2013.

Van Geel, B.: Non-Pollen Palynomorphs, in: *Tracking Environmental Change Using Lake Sediments: Terrestrial, Algal, and Siliceous Indicators*, edited by: Smol, J. P., Birks, H. J. B., Last, W. M., Bradley, R. S., and Alverson, K., Springer Netherlands, Dordrecht, 99–119, https://doi.org/10.1007/0-306-47668-1_6, 2001.

Velichko, A. A., Timireva, S. N., Kremenetski, K. V., MacDonald, G. M., and Smith, L. C.: West Siberian Plain as a late glacial desert, *Quat. Int.*, 237, 45–53, <https://doi.org/10.1016/j.quaint.2011.01.013>, 2011.

1175 Volkova, I. I., Kolesnichenko, L. G., Kirpotin, S. N., Pokrovsky, O. S., and Vorobyev, S. N.: Peat deposits and peat-forming plants in the mires of the West Siberian northern taiga (based on studies of the Khanymei site), *IOP Conf. Ser. Earth Environ. Sci.*, 232, 012018, <https://doi.org/10.1088/1755-1315/232/1/012018>, 2019.

Walvoord, M. A. and Kurylyk, B. L.: Hydrologic Impacts of Thawing Permafrost—A Review, *Vadose Zone J.*, 15, vzj2016.01.0010, <https://doi.org/10.2136/vzj2016.01.0010>, 2016.

1180 Wang, Y., Way, R., Lewkowicz, A. G., Tutton, R., Beer, J., Colyn, V., and Forget, A.: Assessing recent thaw and subsidence of peatland permafrost in coastal Labrador, northeastern Canada, 2023.

Warner, B. G. and Charman, D. J.: Holocene changes on a peatland in northwestern Ontario interpreted from testate amoebae (Protozoa) analysis, *Boreas*, 23, 270–279, <https://doi.org/10.1111/j.1502-3885.1994.tb00949.x>, 1994.

1185 Waskom, M. L.: seaborn: statistical data visualization, *J. Open Source Softw.*, 6, 3021,

<https://doi.org/10.21105/joss.03021>, 2021.

Webb, E. E. and Liljedahl, A. K.: Diminishing lake area across the northern permafrost zone, *Nat. Geosci.*, 16, 202–209, <https://doi.org/10.1038/s41561-023-01128-z>, 2023.

1190 Wei, L., Xu, C., Jansen, S., Zhou, H., Christoffersen, B. O., Pockman, W. T., Middleton, R. S., Marshall, J. D., and McDowell, N. G.: A heuristic classification of woody plants based on contrasting shade and drought strategies, *Tree Physiol.*, 39, 767–781, <https://doi.org/10.1093/treephys/tpy146>, 2019.

Wetterich, S., Rudaya, N., Tumskey, V., Andreev, A. A., Opel, T., Schirrmeister, L., and Meyer, H.: Last Glacial Maximum records in permafrost of the East Siberian Arctic, *Quat. Sci. Rev.*, 30, 3139–3151, 1195 <https://doi.org/10.1016/j.quascirev.2011.07.020>, 2011.

Willis, K. S., Beilman, D., Booth, R. K., Amesbury, M., Holmquist, J., and MacDonald, G.: Peatland paleohydrology in the southern West Siberian Lowlands: Comparison of multiple testate amoeba transfer functions, sites, and *Sphagnum* $\delta^{13}\text{C}$ values, *The Holocene*, 25, 1425–1436, <https://doi.org/10.1177/0959683615585833>, 2015.

1200 Woodland, W. A., Charman, D. J., and Sims, P. C.: Quantitative estimates of water tables and soil moisture in Holocene peatlands from testate amoebae, *The Holocene*, 8, 261–273, <https://doi.org/10.1191/095968398667004497>, 1998.

Zakh, V. A., Ryabogina, N. E., and Chlachula, J.: Climate and environmental dynamics of the mid- to late Holocene settlement in the Tobol–Ishim forest-steppe region, West Siberia, *Quat. Int.*, 220, 95–101, 1205 <https://doi.org/10.1016/j.quaint.2009.09.010>, 2010.

Zhang, H., Amesbury, M. J., Ronkainen, T., Charman, D. J., Gallego-Sala, A. V., and VÄliranta, M.: Testate amoeba as palaeohydrological indicators in the permafrost peatlands of north-east European Russia and Finnish Lapland, *J. Quat. Sci.*, 32, 976–988, <https://doi.org/10.1002/jqs.2970>, 2017.

Zhang, H., VÄliranta, M., Swindles, G. T., Aquino-López, M. A., Mullan, D., Tan, N., Amesbury, M., 1210 Babeshko, K. V., Bao, K., Bobrov, A., Chernyshov, V., Davies, M. A., Diaconu, A.-C., Feurdean, A., Finkelstein, S. A., Garneau, M., Guo, Z., Jones, M. C., Kay, M., Klein, E. S., Lamentowicz, M., Magnan, G., Marcisz, K., Mazei, N., Mazei, Y., Payne, R., Pelletier, N., Piilo, S. R., Pratte, S., Roland, T., Saldaev, D., Shotyk, W., Sim, T. G., Sloan, T. J., Słowiński, M., Talbot, J., Taylor, L., Tsyganov, A. N., Wetterich, S., Xing, W., and Zhao, Y.: Recent climate change has driven divergent hydrological shifts in high- 1215 latitude peatlands, *Nat. Commun.*, 13, 4959, <https://doi.org/10.1038/s41467-022-32711-4>, 2022.

Zhu, X., Xu, X., and Jia, G.: Asymmetrical Trends of Burned Area Between Eastern and Western Siberia Regulated by Atmospheric Oscillation, *Geophys. Res. Lett.*, 48, e2021GL096095, <https://doi.org/10.1029/2021GL096095>, 2021.

Zoltai, S. C.: Cyclic Development of Permafrost in the Peatlands of Northwestern Alberta, Canada, *Arct. Alp. Res.*, 25, 240, <https://doi.org/10.2307/1551820>, 1993.

1220 Zoltai, S. C., Morrissey, L. A., Livingston, G. P., and Groot, W. J.: Effects of fires on carbon cycling in North American boreal peatlands, *Environ. Rev.*, 6, 13–24, <https://doi.org/10.1139/a98-002>, 1998.

